Single Cell Transcriptomics identifies a WNT7A-FZD5 Signaling Axis that maintains Fallopian Tube Stem Cells in Patient-derived Organoids

Abdulkhaliq Alsaadi [1,2,a], Mara Artibani [1,2,3], Zhiyuan Hu [1,2,3], Nina Wietek [1,2,4], Matteo Morotti [1,2,4,b], Laura Santana Gonzales [1,2], Moiad Alazzam [4], Jason Jiang [4], Beena Abdul [4], Hooman Soleymani majd[5], Levi L Blazer [6], Jarret Adams [6], Sachdev S Sidhu [6,7], Joan S. Brugge [8,9] and Ahmed Ashour Ahmed [1,2,4,*]

1 Ovarian Cancer Cell Laboratory, MRC Weatherall Institute of Molecular Medicine, University of Oxford, Oxford OX3 9DS, UK.
2 Nuffield Department of Women's & Reproductive Health, University of Oxford, Oxford OX3 9DU, UK.
3 Gene Regulatory Networks in Development and Disease Laboratory, MRC Weatherall Institute of Molecular Medicine, Radcliffe Department of Medicine, University of Oxford, Oxford OX3 9DS, UK.
4 Department of Gynaecological Oncology, Churchill Hospital, Oxford University Hospitals, Oxford OX3 7LE, UK.
5 Medical Sciences Division, University of Oxford, John Radcliffe Hospital, Oxford OX3 9DU, UK.
6 Donnelly Centre for Cellular and Biomolecular Research, Banting and Best Department of Medical Research, University of Toronto, Toronto, Toronto, Ontario M5S3E1, Canada.
7 Department of Molecular Genetics, University of Toronto, Toronto, Ontario M5S 1A8, Canada.
8 Department of Cell Biology, Harvard Medical School, Boston, MA 02115, USA.
9 Ludwig Center at Harvard, Boston, MA, USA.

[a] Present address: Department of Cell Biology, Harvard Medical School, Boston, MA 02115, USA (abdulkhaliq_alsaadi@hms.harvard.edu)
[b] Present address: Ludwig Institute for Cancer Research, University Hospital of Lausanne (CHUV), Lausanne, Switzerland
* Correspondence: ahmed.ahmed@wrh.ox.ac.uk

ABSTRACT

Despite its significance to reproduction, fertility, sexually transmitted infections and various pathologies, the Fallopian tube (FT) is relatively understudied. Strong evidence points to the FT as the tissue-of-origin of high grade serous ovarian cancer (HGSOC); the most fatal gynaecological malignancy. HGSOC precursor lesions arise specifically in the distal FT (fimbria) which is reported to be enriched in stem-like cells. The role of FT stem cells in HGSOC initiation could not be investigated as these cells have not been identified or functionally characterized due to lack of physiologically relevant models. Here, we surmount technical challenges to re-construct the FT stem cell niche *in vitro.* Using functional approaches as well as bulk and single cell expression analyses, we show that a WNT7A-FZD5 signaling axis is critical for self-renewal of FT stem cells and is regulated by female sex hormones. Single cell expression profiling of reporter organoids identified Wnt/β-catenin Active cells (WβA cells) as a unique cluster of proliferative cells that is enriched in HGSOC markers, particularly *CA125*; a clinical marker of HGSOC progression and response to therapy. Remarkably, we find that the WNT7A-FZD5 signaling axis is dispensable for mouse oviduct regeneration. Overall, we propose a first basic description of the nature of FT stem cells and their molecular requirements for self-renewal, paving the way for mechanistic work investigating the role of stem cells in FT health and disease.

KEY WORDS

Fallopian tube; wnt; ovarian cancer; stem cells; organoids; Estrogen; single cell RNA sequencing

ABBREVIATIONS

hFT	human Fallopian tube
mOV	mouse oviduct
WβS	Wnt/β-catenin Signaling
WβA	Wnt/β-catenin Active
SCT	Single Cell Transcriptomics
KO	Knockout
HGSOC	High Grade Serous Ovarian Cancer

GRAPHICAL ABSTRACT

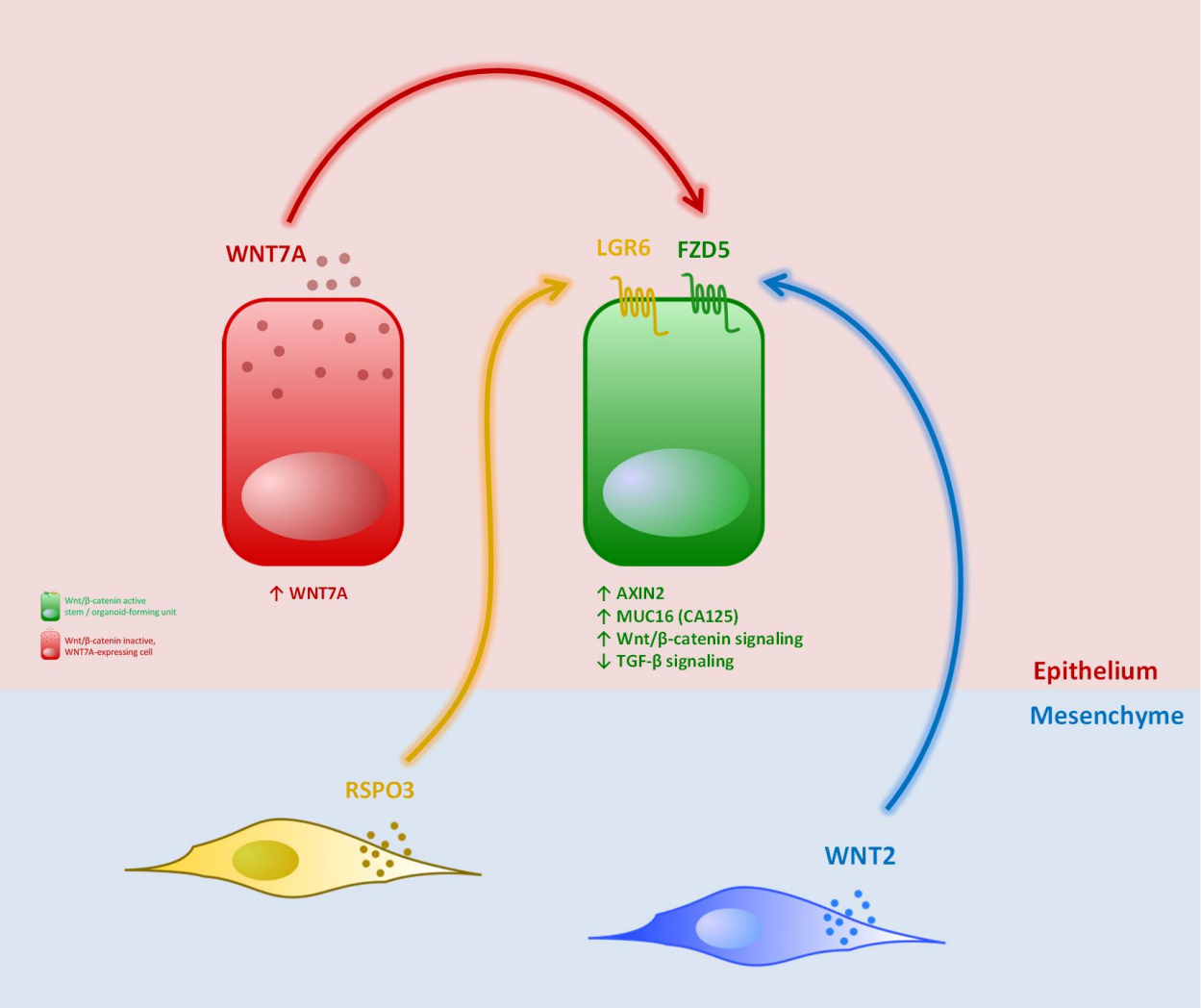

INTRODUCTION

The human Fallopian tube (hFT) is lined with pseudo-stratified columnar epithelium composed of PAX8+ MYC+ secretory cells that nourish released eggs / zygotes, as well as TUBB4+ FOXJ1+ ciliated cells that beat rhythmically to facilitate ovum/zygote transport to the uterine cavity. Despite its significance to fertility, reproduction and women's health and disease, little is known about the FT's biology, cellular hierarchy and homeostasis which are critical for understanding infertility disorders, ectopic pregnancy, sexually transmitted infections and FT-derived cancers. A number of studies have attempted to bridge this knowledge gap, and reports indicate that the distal hFT/mouse oviduct (mOV) is enriched in stem-like cells possessing longevity and multipotency (Erickson *et al*., 2013; Ghosh *et al*., 2017; Xie *et al*., 2018; Wang *et al*., 2012; Zhu *et al*., 2020). In mice, studies identified a population of label-retaining cells (LRCs) at the distal mOV (Snegovskikh *et al*., 2014) that are enhanced for differentiated spheroid formation (Wang *et al*., 2012; Xie *et al*., 2018). Strong evidence for the existence of mOV stem cells came from *in vivo* lineage tracing that employed doxycycline-inducible labelling of secretory cells using a Pax8^{rtTA} TetO^{Cre} YFP$^{fl/fl}$ mouse model. Here, ciliated cells were shown to emerge from secretory cells (Ghosh *et al*., 2017). Similarly, in the hFT putative stem cells were shown to be secretory in nature, using spheroid (Paik *et al*., 2012), air-liquid interface (Yamamoto *et al*., 2016) and organoid-based approaches (Kessler *et al*., 2015).

However, using single cell transcriptomic (SCT) profiling on fresh hFT tissue, we and others have recently uncovered a previously unappreciated heterogeneity within the FT secretory compartment (Hu *et al*., 2020; Dinh *et al*., 2021). Therefore, although *in vivo* studies and human-based *in vitro* models refined the search for hFT/mOV stem cells, no studies have successfully pinpointed the secretory cell type driving FT renewal, due to limitations in model tractability and difficulty in cell biomarking and isolation. Wnt/β-catenin signaling (hereinafter WβS) is thought to be involved in hFT/mOV self-renewal (Kessler *et al*., 2015; Ghosh *et al*., 2017), but the precise molecular mechanisms remain unknown. Furthermore, humans and great apes possess FTs whereas the equivalent in mice is the oviduct. Due to major anatomical differences, biological differences are likely to exist, and no studies have scrutinized whether mOV biology is representative to the hFT.

In addition to being a site where stem-like cells concentrate, mounting evidence from several clinical and *in vivo* studies point to the distal FT fimbria as the site of origin of high grade serous ovarian cancer or HGSOC (Labidi-Galy *et al*., 2017; Kuhn *et al*., 2012; Kim *et al*., 2018). HGSOC is the most fatal gynaecological malignancy with a dismal 5-year survival of 25% that remains persistently low for over four decades (Kroeger & Drapkin, 2017). Understanding FT renewal may shed light on HGSOC initiation mechanisms, which remain poorly understood, further reinforcing the urgency of this investigation. Here, we harness three-dimensional patient-derived FT organoids to reconstruct the FT stem cell niche *in vitro*. We genetically label, isolate and

characterize putative FT stem cells using functional approaches as well as bulk and SCT analyses, identifying a hormonally regulated WNT7A-FZD5 signaling axis that is critical for FT stem cell maintenance.

RESULTS

A serum-free culture method for robust regeneration of hFT organoids from single cells

Multiple models of FT biology were previously reported but each model suffers from drawbacks limiting its utility in characterizing FT stem cells (Figure S1A). In particular, conventional 2D cultures of primary FT cells (Figure S1 B-D) were found to lack ciliated cells (Hu *et al*., 2020) and lose epithelial markers within 5-6 weeks of culture (Figure S1E). Organoid cultures were shown to be robust hFT/mOV models incorporating PAX8+ secretory and TUBB4+ ciliated cells (Kessler *et al*., 2015; Xie *et al*., 2018; Figure 1A), but a major limitation of the human organoid culture conditions is the lack of organoid regeneration after single cell dissociation of patient tissue or organoids; a pre-requisite for isolating and characterizing putative progenitor cells. TGF-β pathway promotes stem cell differentiation (Sakaki-Yumoto *et al*., 2013) and its inhibition is critical for regeneration of organoids from various organs (Sato *et al*., 2009; Bartfeld *et al*., 2015; Karthaus *et al*., 2014; Turco *et al*., 2017). We reasoned NOGGIN, which inhibits BMP-activated SMAD1/5/8-mediated signaling, and SB431542, a TGFβR1 / ALK5 inhibitor which blocks SMAD 2/3 TGFβ-mediated signaling, do not sufficiently inhibit TGF- β signaling to enable organoid regeneration. Thus, we employed A83.01 which has 10-fold higher potency compared to SB431542 (Tojo *et al*., 2005) and found it to restore organoid formation efficiency or OFE (Figure 1 B-C). Interestingly, we found that TGF-β suppression was not necessary for regeneration of mOV organoids from single cells (Figure S2 A-C).

In addition, we excluded WNT3A (Figure S3A) as a WNT source which we show is not needed and has no activity in hFT organoids (see below). Undefined serum factors contained within Wnt3a conditioned medium (CM) negatively interfere with organoid regeneration (Figure S3B) and confound the analysis of stem cell self-renewal requirements *in vitro*. Using this optimized medium, we confirmed that organoids emerge only from epithelial cells (Figure S3C), display invaginations characteristic of hFT tissue (Figure S3D), possess a spherical tube-like structure with a hollow interior (Supplementary Movie 1) and contain a rare population of KI-67+ proliferative cells (Figure S3E). Overall, the data above indicate that we have optimized serum-free culture conditions that robustly support the regeneration of hFT organoids from single cells.

Wnt/β-catenin signaling is essential for renewal of hFT stem cells

FT organoids were previously shown to be monoclonal (Kessler *et al*., 2015). Using our optimised culture conditions, we sought to directly test organoid monoclonality by single cell culture. A small proportion of single cells cultured in single cells formed organoids containing differentiated progeny (Figure 1D), further confirming FT organoids as monoclonal structures emerging from single multipotent stem cells. We set out to characterize these putative stem cells using different approaches (Figure 1E). Our functional analyses above

indicate WβS activation is essential for stem cell renewal in organoids (shown earlier, Figure 1 B-C). To confirm this, we treated organoids with the tankyrase 1/2 inhibitor XAV-939 (Huang *et al*., 2009) and β-catenin / CBP inhibitor PRI-724 (Okazaki *et al*., 2019); both inhibit WβS at midstream (cytoplasmic) and downstream (nuclear) nodes, respectively (Figure S3F). Both treatments completely abolish organoid regeneration (Figure S3G). Furthermore, in our optimized serum-free setting, RSPO1 is the only component that augments WβS (Figure S3H). RSPO1 withdrawal reduces OFE by more than 90% (shown earlier, Figure 1 B-C). Since our culture medium does not contain a WNT source, we reasoned that WβS is activated via an endogenously secreted WNT. Indeed, blocking endogenous WNT secretion in organoids using Porcupine inhibitors (Figure S3I) reduced OFE by over 90% (Figure 1 F-G), phenocopying the effect seen upon RSPO1 withdrawal (show earlier, Figure 1 B-C). This suggested that RSPO1 cooperates with an endogenous WNT to drive hFT organoid regeneration.

WNT3A is a widely employed WNT source in various tissue-derived organoid culture systems, including hFT/mOV organoids (Hoffmann *et al*., 2020; Kessler *et al*., 2015, 2019; Kopper *et al*., 2019; Lõhmussaar *et al*., 2020). We expressed Wnt3a CM using L-Wnt3a cells and validated its activity using the Wnt reporter (TOPFlash) assay (shown earlier, Figure S3A). Contrary to the rescue of organoid regeneration seen in WNT-blocked intestinal organoids (Sato *et al*., 2011), Wnt3a failed to rescue the regeneration of WNT-blocked hFT organoids (Figure 1 H-I), suggesting it cannot substitute for the endogenously secreted WNT ligand. In an unexpected contrast to hFT organoids, the regeneration of mOV organoids was unaffected by blocking endogenous WNTs (Figures 1 J-K), suggesting mouse organoids renew using other mechanisms.

WβS-active cells drive organoid regeneration

The results above indicate that Wnt/β-catenin active (WβA) cells drive FT organoid regeneration.
To characterize WβA cells, we transduced organoids from benign non-HGSOC patients with the 7TGC lenti-construct (Figure 2A). We expanded FACS-selected transduced cells using our optimized culture conditions, to generate stable WβS-reporter organoids (Figures 2B & S4A) from multiple patients. Confocal imaging of fixed (Figure 2C) and live (Figure S4B) organoids confirmed localized activation of WβS in organoids. Immunofluorescence staining confirmed that WβA cells are PAX8+ / secretory in lineage (Figure 2D) and constitute 1.5-5% of all cells (Figure 2E and Figure S4A for mOV and hFT organoids, respectively), mirroring the proportion of organoid-forming units in hFT organoids. Crucially, blocking endogenous WNT secretion abolished EGFP+ cells (Figure 2E) while WβS activation increased the proportion of EGFP+ cells over 10-fold (Figures 2E and S4C), suggesting EGFP faithfully marked WβA cells. AXIN2, a reliable marker of WβS activation in several organoid systems (Boonekamp *et al*., 2021) including hFT organoids (Figure S4D) was elevated in EGFP+ cells (Figure 2F), further validating EGFP+ cells as WβA cells in this setting.

FACS-purified WβA cells displayed enhanced OFE relative to non-WβA cells (Figure 2 G-H). Whilst WβA cells were detected in all organoids within hFT organoid cultures, mOV organoids may or may not contain WβA cells (Figure 2I), and mOV WβA cells do not display enhanced OFE (Figure 2J) under a range of experimental

conditions (Figure S4 F-I), consistent with WβS-independence seen in mOV organoids (shown earlier, Figure 1 J-K).

WNT7A is the driver of WβS and FT stem cell renewal

To identify the WNT ligand driving stem cell-mediated expansion of hFT organoids, we isolated WβA (EGFP+) and non-WβA (EGFP-) cells from WβS-reporter organoids and profiled their transcriptomes at the single cell level using the SMART-seq2 protocol (Picelli *et al*., 2014). This identified *WNT7A* as the highest expressed WNT ligand and the only expressed canonical WNT in hFT organoids (Figure 3A). *WNT7A* expression was further validated using RNAScope FISH staining in hFT organoids (Figure 3B), hFT tissue (Figure S5 A-C), mOV organoids (Figure 3C) and mOV tissue (Figure S5 D-G), showing that *WNT7A*+ cells may or may not co-express WβS activation markers *AXIN2/Axin2* and *LGR5/Lgr5*. Therefore, it is difficult to conclusively say whether WNT7A signals in an autocrine or paracrine manner. However, this data implicates WNT7A as the target of Porcupine inhibitors IWP-2 and LGK-974 which abolish organoid regeneration (shown earlier, Figure 1 F-I). In contrast, *WNT5A* is lowly expressed and is known to be a classic activator of non-canonical Wnt signaling that is β-catenin and LRP5/6-independent (Qian *et al*., 2007). Of note, *WNT3A* expression is not detected in organoids (Figure 3A), suggesting hFT cells are not naturally primed to respond to WNT3A or activate WβS through it. This consistent with WNT3A's failure to rescue growth of WNT-blocked organoids (shown earlier, Figure 1 H-I).

While our data suggests endogenous *WNT7A* provides hFT organoids with independence from exogenously supplied WNTs, we find hFT tissue and organoids express *RSPO1* (Figure 3D) which does not substitute for exogenously supplied RSPO1 in promoting organoid renewal (shown earlier, Figures 1 B-C & F-I). We reasoned another source of RSPOs could be involved *in vivo*. To address this, we surveyed our tissue SCT dataset, which showed that 10% of stromal cells robustly express *RSPO3* (Figure 3E) which biochemical studies indicate is over 20-fold more potent in augmenting WβS compared to RSPO1 (Park *et al*., 2018). Furthermore, 25% of stromal cells express *WNT2* and 7.5% express *WNT9A* (Figure 3E), implying epithelial WNT7A may be a redundant WNT source *in vivo*. Notably, the *WNT2+*, *WNT9A+* and *RSPO3+* stromal cells are largely distinct, and we do not see robust WNT or R-Spondin contribution from the limited number of immune cells profiled (Figure 3E).

Next, we sought to functionally confirm whether WNT7A is essential for renewal of FT stem cells in organoids. Direct genetic knockdown of *WNT7A* mRNA was unsuccessfully attempted using 10 lentiviral shRNA constructs from two commercial sources (data not shown). We also aimed to test whether WNT7A protein rescues OFE of WNT-blocked organoids. In line with the reported difficulties in generating functional WNTs for *in vitro* assays (Tüysüz *et al*., 2017), all generated WNT7A protein reagents were not functional (Figure S6H), including WNT7A CM derived from *WNT7A*-cDNA construct-transfected HEK293 cells (Figure S6 A-B), WNT7A CM from primary 2D-cultured FT cells (Figure S6C) which we find endogenously overexpress WNT7A (Figure S6 D-E), native WNT7A protein (Figure S6G) and recombinant WNT7A protein from two commercial sources (one shown in Figure S6H). Interestingly, the *WNT7A* cDNA expression construct robustly activates WβS but the CM

derived from the same construct-transfected cells fails to activate WβS (Figure S6H), despite containing abundant WNT7A protein (shown earlier, Figure S6 A-B). We reasoned this could be due to a short signaling range as shown by biochemical and *in vivo* approaches for other WNT ligands (Farin *et al*., 2016; Goldstein *et al*., 2006; Alexandre *et al*., 2013). We confirmed this using a simple co-culture assay (Figure S6 I-J); 4E), which explained why our protein-based WNT7A reagents were not functional.

FZD5 mediates WNT7A-driven maintenance of FT stem cells

To overcome the above limitations and test the functional significance of WNT7A to organoid renewal, we attempted to identify and biochemically perturb the WNT7A receptor in organoids. SCT profiling identifies *FZD3*, *FZD5* and *FZD6* as the major FZDs expressed in hFT organoids (Figure 4A). This is also the case for hFT tissue (Figure S7A). The FZD family of receptors categorize into 4 subfamilies based on sequence and structural similarity: FZD5/8 subfamily, FZD4/9/10 subfamily, FZD1/2/7 subfamily and FZD3/6 subfamily. The FZD3/6 subfamily is the divergent one from this receptor family (Figure S7B) and participates in non-canonical Wnt signaling (Dong *et al*., 2018). FZD5, and not FZDs 3/6, was reported to bind WNT7A and activate WβS as shown in *in vitro* WNT-FZD pair screens (Yu *et al*., 2012; Voloshanenko *et al*., 2017). To validate these findings, we utilized HEK293 cells which endogenously express these FZDs (Figure S7C). siRNA knockdown (Figure S7D) of *FZD5*, but not *FZD3* or *FZD6*, inhibited *WNT7A*-induced TOPFlash (Figure S7E) while WNT7A induced the highest WβS/TOPFlash signal in a background of FZD5 overexpression compared to FZD3 or FZD6 overexpression (Figure S7F).

Although this data confirms WNT7A activates WβS through FZD5, direct functional evidence from hFT organoids is lacking. To address this, we utilized IgG-2919 and IgG-2921; two novel, selective, antibody-based inhibitors of FZD5 generated using an antibody phage-display system (Steinhart *et al*., 2017). Anti-FZD5 IgGs reduce TOPFlash signal in WNT7A and FZD5 overexpressing cells by more than 60% (Figure S7G). Consistent with WNT inhibition's dual effect on abolishing WβA cells (shown earlier, Figure 2E) and OFE (shown earlier, Figure 1 F-I), FZD5 inhibition abolishes WβA cells (Figure 4B) and OFE (Figure 4C) by over 90% (Figure 4D). This phenocopies the effect of RSPO1 withdrawal (shown earlier, Figure 1 B-C & 1 F-I). The only other FZD that shows cross-reactivity with anti-FZD5 antibodies is FZD8 (Figures 3C & S5 in Steinhart *et al*., 2017) which is not expressed in hFT organoids (shown earlier, Figure 4A). Altogether, these data strongly suggest that FZD5 is the cognate receptor for WNT7A in the FT, and that a WNT7A-FZD5 signaling axis drives WβS activation and renewal of hFT organoids.

Regeneration of FZD5-inhibited or WNT-blocked organoids is rescued by WβS activation downstream of ligand-receptor interactions using the selective GSK-3β inhibitor CHIR99021 (Figure 4 C-D). Partial rescue is also observed when WβS is activated at the ligand-receptor level using Surrogate Wnt (Figure 4 C-D), which competes with anti-FZD5 IgG's for binding to FZD's cysteine-rich domain (Janda *et al*., 2017; Steinhart *et al*., 2017). Surrogate Wnt has broad-spectrum activity against FZDs 1/2/5/7/8 but not FZDs 3/6 (Janda *et al*.,

2017), further demonstrating that FZD5 is the FZD receptor associated with WβS and organoid regeneration. FZD receptors are subject to constant turnover and proteasomal degradation by the action of the RNF43/ZNRF3 ubiquitin ligases (Hao *et al*., 2012), which are inhibited by R-Spondins (Carmon *et al*., 2011; Glinka *et al*., 2011; de Lau *et al*., 2011). As such, withdrawal of RSPO1 from Surrogate Wnt-treated organoids reduces OFE by 75-90% (Figure 4E), indicating that the reduced OFE seen upon RSPO1 withdrawal (shown earlier, Figures 1 B-C & 1 F-I) is due to FZD5 turnover.

Intriguingly, while organoids from all tested patients in this study showed sensitivity to WβS inhibition, organoids from one patient were resistant to WNT and FZD5 inhibition (Figure S8 A-B) as well as to RSPO1 withdrawal (Figure S8C). Patient 5 organoids were, however, sensitive to downstream WβS inhibition (Figure S8 A-B) as seen in other patients (shown earlier, Figure S3G). Tested under selective conditions of WNT-blocking for four passages, Patient 5 organoids show ectopic and robust growth that leads to large organoid sizes not typical of normal FT organoids (Figure S8D). Although Patient 5 was diagnosed with serous ovarian cancer, which is thought to derive from the FT (Kuhn *et al*., 2012; Kim *et al*., 2018), Patient 5 organoids do not carry TP53 mutations, which are known to be the initiating event of serous ovarian cancer (Labidi-Galy *et al*., 2017). While further characterization and more patient replicates are required to reproduce this finding, these WNT/FZD5-resistant organoids may represent purified mutant clones with early genetic changes that confer selective growth advantage and independence from stem cell niche requirements.

Finally, FZD5 inhibition has no effect on mOV organoids (Figure 4 F-G) consistent with the lack of effect seen upon blocking WNT secretion (shown earlier, Figure 1 J-K) and lack of OFE enrichment in isolated WβA mOV cells (shown earlier, Figure 2J). This is despite WNT blocking and FZD5 inhibition abolishing WβA cells in mOV WβS-reporter organoids (shown earlier, Figure 4B), suggesting that a WNT-FZD5 signaling axis also regulates WβS in mOV organoids, but unlike in hFT organoids, WβS is not essential for stem cell renewal in the mOV organoids.

Estrogen downregulates WNT7A and triggers ciliogenesis

Female Reproductive Tract (FRT) organs, including the hFT/mOV, are subject to cyclic hormonal influences. Estrogen acts as a ligand that dimerizes Estrogen receptors (ER) expressed in cells within hormone-responsive tissues (Björnström & Sjöberg, 2005). Little is known about Estrogen's influence on WβS in the hFT, and studies indicate Estrogen activates WβS in the FRT (Hideyuki *et al*., 1999; Kouzmenko *et al*., 2004; Hou *et al*., 2004) although other reports document Estrogen to exert an inhibitory influence on WNT7A (McLachlan *et al*., 1980; Couse *et al*., 2001; Wagner & Lehmann, 2006). Based on this, it can be hypothesized that Estrogen may uncouple the synonymous and proportional relationship we see between WβS and WNT7A in the FT.

To evaluate this hypothesis, Estrogen's and Progesterone's effects on WβS were tested in the presence of Estrogen Receptor (ERα) and Progesterone Receptor (PRβ), respectively. Interestingly, Estrogen robustly

activates transcription from WβS Reporter Elements (or WβS-RE) in the TOPFlash assay (Figure S9A), independently of WNT ligands (Figure S9B). Estrogen's activation of transcription at WβS-RE elements is unaffected by WβS inhibitors at midstream (XAV-939) and downstream (PRI-724) levels (Figure S9B). Estrogen also attenuates ligand-dependent and ligand-independent hyperactivation of WβS (Figure S9C) to levels seen in Estrogen-treated samples (Figure S9A), indicating that the E2-ERα complex may compete or cooperate with β-catenin for binding and activation at WβS-REs. To test this, we investigated the effect of Estrogen on TOPFlash signal upon β-catenin knockdown. β-catenin siRNAs were validated to effectively abolish β-catenin protein levels (Figure S9D) and activity (Figure S9 E-F). In this setting, liganded ERα activates transcription at WβS-RE elements independently of β-catenin (Figure S9G) and induces WβS target gene transcription 45-88% higher in the absence of β-catenin, suggesting the pair compete for binding at WβS-RE promoter elements. Next, we sought to delineate the effect of Estrogen on WNT7A. Interestingly, Estrogen (as well as Progesterone) causes degradation of intracellular and secreted WNT7A protein (Figure 5A), and dramatically reduces WNT7A activity (Figure 5B) without independently activating WβS (as shown earlier; Figure S9A). Overall, these data suggest that Estrogen can activate WβS target gene expression in hormone-responsive tissues, but specifically suppresses WNT7A and WNT7A-induced WβS in the FT setting.

Estrogen's differential effects on WβS and WNT7A are interesting. They were confirmed here using the TOPFlash assay which, although useful, is not physiologically relevant to the FT. Organoids offer a superior model to understand hormonal control of WβS and WNT7A, and SCT data confirms that our optimized organoid culture conditions successfully maintain hormone receptor-expressing cells (Figure 5C) as seen in human tissue (Figure 5D). In both settings, ERα is the predominant hormone receptor expressed, and we harnessed this model to understand Estrogen's influence on the FT. Estrogen treatment of hFT organoids triggers a phenotype of crippled, deeply staining organoids with extensive internal folding and invaginations (Figure 5 E-F), reminiscent of differentiation signs that appear in long-term cultured organoids (shown earlier, Figure 1D) and in differentiated organoids of other tissues (Yin *et al*., 2013). However, Estrogen triggers these changes within 72 hrs, and characterisation of Estrogen-treated organoids reveals Estrogen downregulates *WNT7A* expression, WβS and the proliferation marker Ki-67 (Figure 5 G-H). Furthermore, we detect upregulation of *FOXJ1*, an established master regulator and marker of ciliated cells (You *et al*., 2004), as well as upregulation of *CAPS*, *CCDC17*, *CCDC78* (Figure 5I) and *CCDC78* (Figure S9H); all novel ciliated cell markers we previously identified in a tissue-based SCT study (Hu *et al*., 2020).

Finally, WβS was recently shown to regulate the expression of DNA double-strand break repair genes, including *BRCA1*, *BRCA2*, *RAD51* and the *FANC* gene family, in various tissues (Kaur *et al*., 2021; Angers, 2021). Along with inhibiting WβS, we note Estrogen suppresses *BRCA1* and *BRCA2* expression in hFT organoids, possibly through *MYBL2* (Figure S9I) as reported (Kaur *et al*., 2021). This is phenocopied by Estrogen-independent WNT inhibition (Figure S9I), suggesting Estrogen regulates *BRCA1/2* expression, at least in part,

through regulating WβS. Collectively, the data indicates that Estrogen suppresses *WNT7A* and WβS, and robustly induces a transcriptional ciliogenesis programme in hFT organoids.

Transcriptomic characterization of WβA cells

Our data thus far reveal a hormonally-regulated WNT7A-FZD5 signaling axis that activates WβA cells which drive FT organoid regeneration. WβA cells are therefore candidate FT stem cells, which we sought to further characterize using our expression dataset which profiled WβA and non-WβA cells at the single cell level. Among the four transcriptomic clusters identified (Figure 6A) WβA cells concentrate in cluster 1 (Figure 6B; p-values for pairwise WβA cell enrichment in cluster 1 relative other clusters is < 0.0002; see Figure 6C). Cluster 1 cells are enriched in the expression of cell cycle and mitosis-related genes (Figure 6D), and a full list of cluster-based DEGs is available (Table S1). We also compared WβA with non-WβA cells irrespective of cluster position. Table S2 provides a full list of WβS status-based DEGs. Interestingly, *WNT7A* expression is enriched in the proliferative WβA cells (Figure 6E; p-value < 10^{-6}). In hFT tissue, we also find *WNT7A*+ cells to be proliferative (data not shown) and transcriptionally unique (Figure 6F). Next, we aimed to identify the RSPO1 receptor which is responsible for the obligate RSPO1 requirement for hFT organoid regeneration (shown earlier, Figure 1 B-C & F-I). Since our organoid SCT data does not capture the expression of R-Spondin receptors (LGRs 4-6) possibly due to dropout of low abundance mRNAs, we carried out bulk RNA-seq of WβS-reporter organoids. This further confirmed upregulation of WβS in WβA cells (Table S3) and identified *LGR6* as the only R-Spondin receptor enriched in WβA cells (Figure 6G).

Further analysis of our organoid SCT data revealed Dipeptidyl peptidase 4 (*DPP4*) expression is enriched in WβA cells (Figure 6H; p-value < 10^{-9}). DPP4 is a transmembrane enzyme involved in glucose and insulin metabolism (Ghorpade *et al*., 2018; Röhrborn *et al*., 2015) and was recently shown to mark WβA cells *in vivo* in the endometrium (Syed *et al*., 2020), which shares an embryonic origin and a developmental continuum with the mOV, corroborating our findings. Interestingly, WβA cells are enriched in *MUC16* expression (Figure 6H; p-value 0.0017). MUC16, also called CA125, is highly overexpressed in HGSOC tumours (Bast *et al*., 1983) and is a clinically established biomarker for patient diagnosis, disease progression and response to therapy (Partridge *et al*., 2009). WβA cells are also marked by *GPX3* (Figure 6H, p-value < 10^{-8}), an extracellular glutathione peroxidase that protects cells against oxidative damage and was shown to support ovarian cancer invasion and survival (Worley *et al*., 2019). Finally, Claudin-3, a tight junction protein highly overexpressed in ovarian cancer (Rangel *et al*., 2003) and proposed to better diagnose CA125^{low} ovarian cancers (Rosen *et al*., 2005) also marks the WβA cluster (Figure 6H; p-value < 10^{-7}). Collectively, our organoid SCT data suggests that WβA cells are unique, and their proliferative capacity is consistent with progenitor cell character. The observation that WβA cells are marked by *CA125* and other HGSOC markers may implicate these cells in HGSOC initiation, representing an attractive future research direction that warrants investigation.

DISCUSSION

The first organotypic culture techniques for human Fallopian tube (hFT) and mouse oviduct (mOV) tissues were described relatively recently (Xie *et al*., 2018; Kessler *et al*., 2015), and a number of studies have utilized this to make important progress in understanding FT and HGSOC biology (Zhang *et al*., 2019; Lõhmussaar *et al*., 2020; Kessler *et al*., 2019; Kopper *et al*., 2019; Hoffmann *et al*., 2020; Hill *et al*., 2018; de Witte *et al*., 2020). Organoids emerge from single multipotent cells in bulk and single cell culture, and we find ciliated cells appear several days after organoid passage (data not shown), consistent with *in vitro* (Kessler *et al*., 2015) and *in vivo* (Ghosh *et al*., 2017) studies showing ciliated cells emerge from secretory cells. Although this strongly points to the presence of a stem cell, no studies have thus far harnessed hFT organoids for stem cell expansion and characterization. This is due to limitations in published protocols in which culture conditions are poorly defined and in their current format are not amenable to single cell isolation and culture.

In this study, we develop serum-free culture conditions enabling stem cell expansion from single cells. We confirm that organoids grown under these conditions recapitulate basic features of hFT tissue, and have recently extended this to detect, in organoids, novel cell types and markers identified by the first single cell transcriptomic (SCT) study on hFT tissue (Hu *et al*., 2020). We harness our optimized culture conditions to conduct functional analyses on molecular determinants of stem cell renewal, and devise a strategy for marking, isolation and transcriptomic characterization of these cells, generating the first SCT dataset of hFT organoids.

WNT7A, FZD5 and RSPOs in the hFT: Our work implicates WNT7A in FT homeostasis and maintenance. This is consistent with *in vivo* studies that reported *Wnt7a* knockout (KO) mice to contain no or severely compromised mOV with diminished invaginations, as well as global abnormalities in the correct patterning of the neonatal female reproductive tract or FRT (Miller & Sassoon, 1998). Although viable, *Wnt7a* KO mice are reproductively sterile and the Mullerian duct fails to regress in male mice (Parr & McMahon, 1998). WNT7A is known to play an intimate role in patterning and differentiation of other tissue types, including limb, cardiac and neuronal synapses (Bond *et al*., 2003; Ingaramo *et al*., 2016; Hwang *et al*., 2004; Hall *et al*., 2000).

Our data shows strict concordance between the proportion of Wnt/β-catenin Active (WβA) cells and organoid renewal capacity, both in the range of 1.5-5% of cells. We note non-WβA cells may also generate differentiated organoids, consistent with regenerative plasticity seen in organoids derived from FRT organs (Ali *et al*., 2020; Syed *et al*., 2020) and other tissues (Serra *et al*., 2019; Huch, Bonfanti, *et al*., 2013; Sato *et al*., 2009; Cao *et al*., 2020). Our data shows that LGR6, and not FZD5, is enriched in WβA cells, and we hypothesize that LGR6 is the limiting factor in dictating multipotency of WβA *FZD5*+ *LGR6*+ cells. A limitation of our work is

the lack of functional analyses to evidence this. Furthermore, our tissue SCT data indicates epithelial WNT7A could be made redundant by mesenchymal-derived WNTs, offering an explanation as to why conditional *Wnt7a* loss does not disrupt mOV homeostasis *in vivo* (Dunlap *et al*., 2011). As FZDs 3/6 are largely non-canonical Wnt signaling mediators (Dong *et al*., 2018), we propose mesenchymal-derived WNT2 also signals through FZD5, consistent with *in vitro* WNT-FZD pair screens showing WNT2 activates WβS through FZD5 but not FZDs 3/6 (Yu *et al*., 2012). Unlike epithelial-derived WNT7A, we hypothesize epithelial-derived RSPO1 is not sufficient for hFT homeostasis, and our patient stroma SCT data hints at the possibility that the FT epithelium relies on the mesenchyme as an essential source of RSPO3 necessary for epithelial homeostasis. Another limitation of our work is the absence of WNT2 and RSPO3 in our functional analyses.

Overall, we propose a first description of the FT stem cell niche (Figure 7A). Our transcriptomic and RNA FISH data suggest *WNT7A* expression overlaps (but not completely) with WβA cells, so it is possible that WNT7A signals in an autocrine manner (Figure 7B). Further biochemical work is required to conclusively establish the mechanism of WNT7A signaling in the FT.

WβA cells and mouse models: WβS is recognized as a major driver of tissue regeneration under homeostatic and injury conditions (Clevers, 2006). Amongst various WβS reporters, AXIN2 and LGR5 are the most faithful (Boonekamp *et al*., 2021) and as such, AXIN2 and LGR5-based mouse models have been employed in biomarking and lineage tracing of WβA stem cells in various tissues (Clevers, Loh & Nusse, 2014; Van Camp *et al*., 2014). To this end, *Lgr5*+ cells were shown to contribute to mOV development, but *Lgr5* expression disappears by day 7 after birth (Seishima *et al*., 2019) and in adult mice lineage tracing studies have shown that *Lgr5*+ cells do not contribute to mOV homeostasis (Ng *et al*., 2014). This is consistent with our bulk transcriptomic analysis showing that WβA cells are not enriched in *LGR5* expression.

Although *Lgr5* specifically markers homeostatic WβA-ASCs in various tissues (Barker & Clevers, 2010), including the pyloric stomach (Barker *et al*., 2010) in which *Axin2*+ *Lgr5*- cells are facultative ASCs mobilized upon injury (Sigal *et al*., 2017), the opposite trend is seen in other tissue systems in which AXIN2 is a better marker of homeostatic WβA-ASCs. This was shown in the liver (Wang *et al*., 2015; Huch *et al*., 2013), stomach (corpus) region (Stange *et al*., 2013; Leushacke *et al*., 2017) and adult vagina (Ali *et al*., 2020; Ng *et al*., 2014). In the endometrium, which shares embryonic origins and a developmental continuum with the mOV, *Lgr5*+ cells contribute to development but not adult tissue homeostasis (Seishima *et al*., 2019), and *in vivo* lineage tracing has demonstrated *Axin2*+ cells to be long-lived multipotent stem cells that replenish glandular and luminal epithelia in the adult endometrium (Syed *et al*., 2020). This, coupled with our transcriptomic analyses showing *AXIN2* and *LGR6* are preferentially enriched in WβA cells, as well as our human and mouse RNA FISH data suggesting that *AXIN2*+/*Axin2*+ and *LGR5*+/*Lgr5*+ cells are largely distinct, suggests that alternative WβA tracing strategies should be investigated before conclusively ruling out a role for WβA cells in hFT/mOV

homeostasis. In this regard, we propose *Axin2* as a strong candidate for marking putative multipotent mOV progenitors, as well as *Lgr6* which we find to be the only RSPO receptor enriched in WβA cells.

These proposed *in vivo* investigations are conditional on resolving inter-species differences highlighted in this study. It was previously shown that regeneration of mOV organoids is WβS-independent (Lõhmussaar *et al*., 2020). We extend this observation to show that a WNT-FZD5 signaling axis also regulates WβS in mOV organoids, and RNA FISH staining confirms presence of *Wnt7a+* cells in mOV tissue and organoids. However, unlike in the human setting, inhibition of this signaling axis (which depletes the WβA cell compartment) has no effect on mOV organoid regeneration, and isolated WβA cells do not display enhanced OFE under a range of tested conditions. Similarly, TGF-β signaling inhibition, which is essential for hFT organoid renewal, is dispensable for mOV organoid regeneration. We find these differences to be striking and warrant further investigation, particularly to address whether these deviations represent a biological inter-species difference or are the result of *in vitro* culture conditions.

Hormonal regulation of the FT stem cell niche: Estrogen has been reported to promote WβS and proliferation in FRT tissues (Kouzmenko *et al*., 2004; Hou *et al*., 2004; Gunin *et al*., 2004; Polotsky *et al*., 2009) but the molecular details of this mechanism remain poorly defined. We report novel findings that suggest Estrogen-ERα surpasses the cellular WβS machinery to activate transcription of WβS target genes. In the presence of WNT7A, however, we note Estrogen signaling negatively regulates WNT7A protein and WNT7A-induced WβS, and in hFT organoids Estrogen downregulates *WNT7A* at the mRNA level. This is consistent with reports showing that W*NT7A/Wnt7a* expression drops in the endometrium during the Estrogenic phase of the menstrual cycle in humans (Bui *et al*., 1997) and mice (Miller *et al*., 1998). Our data is also consistent with *in vivo* studies in which treatment of mice with Diethylstilboestrol (DES; an Estrogen analogue) phenocopies the above-described *Wnt7a* KO phenotypes (McLachlan *et al*., 1980) and downregulates *Wnt7a* mRNA levels in the neonatal FRTs (Miller *et al*., 1998). This downregulation is absent in ERα KO mice (Couse *et al*., 2001) further confirming this is an estrogenic effect. Clinically, human patients exposed *in utero* to DES showed similar phenotypes to *Wnt7a* KO mice, including FT abnormalities, lack of tubal coiling, withered Fimbria and infertility (DeCherney *et al*., 1981).

The molecular mechanism of Estrogen's suppression of WNT7A remains unclear. However, *in vivo* studies of the endometrium suggest mesenchymal WNT5A, activated by ER+ fibroblasts, mediate Estrogen's suppression of *Wnt7a*, either by DES treatment or during the Estrogen-dominated phase of the estrous cycle (Mericskay, Kitajewski, & Sassoon, 2004). As WNT5A is a documented inhibitor of WβS via non-canonical Wnt signaling (He *et al*., 2008; Olson & Gibo, 1998; Topol *et al*., 2003), we propose it exerts its influence through epithelial FZDs 3/6. Although we do not detect ER+ WNT5A+ cells in our patient stroma SCT dataset, it is plausible that aged patients (which constitute the bulk of our patient cohort) do not activate mesenchymal WNT5A expression due to menopausal absence of Estrogen, and further investigation of samples from premenopausal hormone-

exposed cohorts is required to ascertain this. Overall, we propose a working model for hormonal regulation of the proposed FT stem cell niche (Figure 7C).

An inherent limitation of this model is the notion of modelling Estrogen's complex interactions *in vitro*. Cells are known to elicit differential responses to Estrogen depending on its local concentration, and the cyclic nature and physiological doses of Estrogen *in vivo* are difficult to recapitulate *in vitro*. The phenotypes observed in Estrogen-supplemented organoids, therefore, while providing a preliminary understanding of Estrogenic molecular changes, are likely not to capture the full spectrum of molecular and phenotypic changes induced by Estrogen *in vivo*. Another limitation of our work is the absence of the stroma in our organoid model, precluding the study of estrogenic stromal changes that regulate mesenchymal-to-epithelial signaling. To address this, we propose the optimization of complex FT organoid co-cultures methods incorporating stromal and other microenvironmental components to dissect these changes as well as study the effect of mesenchymal-derived factors such as WNT2, RSPO3 and TGF-β inhibitors, and their influence on the FT stem cell niche.

WβA cells & HGSOC: High Grade Serous Ovarian Cancer (HGSOC) is a public health burden and the main driver of high mortality in ovarian cancer. Serous Tubal Intraepithelial Carcinomas (or STICs) are thought to be HGSOC's precursor lesion, and were documented in sporadic HGSOC (Howitt *et al*., 2015; Chen *et al*., 2017) and germline BRCA-associated HGSOC (Howitt *et al*., 2015; Finch *et al*., 2006). STICs display an unusually specific localization to the distal FT (Crum, 2009); a region enriched in stem-like cells (Wang *et al*., 2012; Zhu *et al*., 2020; Erickson *et al*., 2013; Xie *et al*., 2018) and active WβS (Ghosh *et al*., 2017). Interrogation of the role of these cells in HGSOC initiation has been hampered by lack of knowledge about FT stem cells, and lack of reliable FT models.

In this work, we report that WβA FT cells from non-HGSOC patients possess unique transcriptomes featuring a number of established HGSOC markers. WβA FT cells are also marked by *WNT7A,* which was shown using orthotopic and subcutaneous xenograft models to drive HGSOC proliferation, invasion and metastatic dissemination throughout the peritoneal cavity (Yoshioka *et al*., 2012; King *et al*., 2015). High *WNT7A* expression was correlated with high *CA125* expression in HGSOC samples (Zhang *et al*., 2010), consistent with our transcriptomic analysis showing co-enrichment of *WNT7A* and *CA125* in WβA cells. In this regard, one hypothesis we propose is that WβA cells possess enhanced self-renewal capacity and may be primed to be the targets of early HGSOC-initiating mutations that produce precursor STIC lesions, which subsequently progress to advanced HGSOCs that retain the expression of these markers. Furthermore, recent studies show that WβS regulates expression of DNA double-strand break repair genes via a WβS/MYBL2 signaling axis (Kaur *et al*., 2021; Angers, 2021). This includes *BRCA1* and *BRCA2* genes, which are of clinical relevance to HGSOC initiation. Our work is a first report suggesting applicability of this regulation axis to the hFT setting. It is tempting to speculate, based on these findings, that WβA cells are enriched in *BRCA1/2* expression, and that *BRCA1/2* loss

preferentially targets WβA cells in HGSOC initiation. Notably, although we see robust reduction of *BRCA1/2* expression upon WNT inhibition, we do not observe enhanced *BRCA1/2* levels in WβA cells isolated from our WβS-reporter organoids. This could be due to endogenous WβS levels, which are higher *in vivo* compared to our organoid setting (Figure S4E), possibly due to contribution from mesenchymal WNTs and RSPOs *in vivo*. Overall, FT WβA cells may be preferential targets of *BRCA1/2* mutation and possibly HGSOC initiation, and more detailed molecular investigation is needed to conclusively establish this.

In conclusion, we propose a first basic description of the character of FT stem cells and their molecular niche requirements for homeostasis. Our work lays the foundation for subsequent functional and *in vivo* studies on FT homeostasis, disease, hormonal regulation and epithelial-mesenchymal crosstalk. Our findings provide a basis for mechanistic work investigating the role of FT stem cells in ovarian cancer initiation.

MATERIALS & METHODS

Human FT clinical samples

Fallopian tube tissue samples were obtained from patients undergoing cancer surgery at the Department of Gynaecological Oncology, Churchill Hospital, Oxford University Hospitals, United Kingdom. Patients were appropriately informed and consented, and cases were recruited as part of the Gynaecological Oncology Targeted Therapy Study 01 (GO-Target-01, Research Ethics Approval #11-SC-0014, Berkshire NRES Committee), as well as under the Oxford Centre for Histopathology Research (OCHRe) / Oxford Radcliffe Biobank (ORB) research tissue bank ethics reference 19/SC/0173.

Mouse Tissue samples

All mouse tissue samples were harvested and provided by the Biomedical Sciences Facility, University of Oxford. Mouse colonies were maintained in certified and licensed animal facilities and in accordance with the United Kingdom's Home Office Animals (Scientific Procedures) Act 1986. All personnel handling animals hold Home Office-issued Personal Licenses. Tissues were obtained from female mice, strain C57BL/6 and aged 7-12 weeks.

Tissue Dissociation & Primary Culture

Primary tissue was washed and cut longitudinally to expose the epithelium. Tissue was dissociated using pre-warmed Digestion medium containing 2 mg/ml Trypsin (Sigma), 0.5 mg/ml DNase I (Sigma) and 100 U/ml Collagenase Type I (Invitrogen) for 45 min to 1 hour at 37 ^{0}C in constant rotation. Cells were passed through a 70, 100 or 250 µm cell strainer and pelleted by centrifugation at 300 g / 5 min / 4 ^{0}C, washed with cold DPBS and used for downstream analysis. For standard 2D culture, isolated cells were resuspended in BM2 culture medium containing Advanced DMEM/F12 (ThermoFisher), 12 mM HEPES (ThermoFisher), 5% FBS (GIBCO), 1% Penicillin/Streptomycin (GIBCO), 100 ng/ml EGF (ThermoFisher) and 10 µM Y-27632 (ROCK inhibitor, Sigma), as described (Kessler *et al*., 2015). For patient tumour samples, the processing protocol was similar but utilized the Tumour Digestion Kit (Miltenyi Biotech), and digestion was performed for 2 hrs at 37 ^{0}C.

Human FT Organoid Culture

To establish human FT organoids, processed cell pellet was resuspended in Extracellular Matrix (ECM, Matrigel, Corning), plated as 50 µl drops on pre-warmed culture plates and incubated at 37 ^{0}C for 20-30 min to allow Matrigel polymerization. After that, cells were overlaid with pre-warmed Organoid Medium containing BM2 medium above (no FBS), supplemented with 100 ng/ml human Noggin (Peprotech), 100 ng/ml human Fibroblast Growth Factor-10 (FGF-10, Peprotech), 1% N2 supplement (ThermoFisher), 2% B27 supplemented (ThermoFisher), 1 mM Nicotinamide (Sigma), 1 mM N-acetyl L-cysteine (Sigma), 5 µM A83-01 (Tocris), 10 µM

Forskolin (Tocris) and R-Spondin 1, which was obtained either commercially (Peprotech) or produced in-house using a HA-RSPO1-Fc 293T cell line. Surrogate Wnt (ImmunoPrecise) was used wherever indicated. 10 µM Y-27632 (Tocris) was added for the first 2-3 days of organoid culture and removed in the first medium change, until the next passage. WNT3A conditioned medium was generated using L-WNT3A cells (ATCC), validated using the TOPFlash assay and used in the indicated experiments.

For maintenance of hFT organoids, organoids were passaged at a ratio of 1:3 to 1:5 every 10-14 days. Briefly, organoids were released from Matrigel by incubation with Organoid Harvesting Solution (Culturex) at 4 ^{0}C in rotation, for 45-90 min. Organoids were then collected into a 15 mL or 50 mL falcon tube, pelleted by centrifugation at 300 g / 10 min / 4 ^{0}C, washed with cold PBS once and used for passage or flow/FACS-related downstream analysis. For passage, dissociation was performed by mechanically shearing organoids using a p200 pipette. For flow analysis or FACS sorting, single cell dissociation was performed by resuspending organoids in pre-warmed 7.5X TrypLE Express (ThermoFisher) diluted in Organoid Wash Buffer (OWB), for 5-10 min. OWB buffer is composed of complete organoid medium + Y26632 but lacking growth factors (EGF, FGF-10, Noggin and RSPO1). Organoids (now single cells) were then washed twice with cold PBS and utilized for FACS or single cell culture. For cryopreservation, pelleted organoids were mechanically fragmented, embedded in Recovery Cell Culture Freezing Medium (ThermoFisher), transferred to -80 ^{o}C freezer overnight and finally transferred to Liquid Nitrogen for long-term storage. For culture re-establishment after cryopreservation, thawed organoids were resuspended in 9 ml OWB buffer, pelleted, washed and cultured in a well of a 24-well plate, as described.

Mouse Oviduct Organoid Culture and passage

Mouse Oviduct, mammary or epidermal organoids were established from primary tissue as described above for hFT organoids. Culture medium for mouse organoids was the same as hFT organoids, excluding A83.01 and Forskolin. Mouse organoids were passaged as reported (Xie *et al*., 2018).

Organoid Formation Efficiency assay

OFE analysis was performed on single cell dissociated tissue or organoids. Single cells were derived as described above. After quantifying cell number, cells were resuspended in Matrigel and plated as Matrigel drops in wells of a 24-well plate. Different wells were subjected to different treatments for 7-12 days. OFE was estimated as number of organoids emerging from the total number of cultured cells per well. For experiments requiring FACS isolation of FT cells, cells were prepared for FACS by cold PBS washing followed by blocking non-specific antibody staining using FcR Blocking Reagent (Miltenyi) for 10 min in the dark in a fridge. Further antibody incubation was performed using CD45-FTIC and EpCAM-APC (Biolegend), in a total volume of 100 µl volume. WβS-reporter organoids (see below) were FACS isolated using mCherry gating, and non-transduced parental organoid lines were used here as negative controls. FACS isolated cells were sorted directly into Matrigel, cultured for 10-14 days and OFE quantified as described.

Generation of Wnt/β-catenin signaling reporter organoids

To generate WβS-reporter organoids, viral lenti-particles were generated by transfecting HEK293 cells in a T25 flask with 15 µg of the lentiviral WβS-reporter construct (7TGC; Addgene #24304), 15 µg envelope plasmid (pMD2.G, Addgene #12259) and 15 µg packaging plasmid (psPAX2, Addgene #12260) using the Lipofectamine 3000 protocol (ThermoFisher). WβS-reporter construct was a gift from Roel Nusse (Fuerer & Nusse, 2010; see Figure 2C for map). Envelope and packaging plasmids were gifts from Didier Trono. Viral supernatant was concentrated using the Lenti-X Concentrator (Takara). Target cells were transduced in complete culture medium containing 8 ug/ml polybrene, for 72 hrs. Upon FACS selection, organoid culture was established and expanded from transduced cells, for 6-12 weeks. WβS-reporter organoids can be made available upon request.

Single cell RNA-sequencing of Wnt/β-catenin reporter organoids

Single cell RNA sequencing (scRNA-seq) was performed on low passage hFT WβS-reporter organoid lines. Organoids were harvested on days 8-11 as described above (including RNasin Plus RNase inhibitor, Promega). Single cell dissociation was performed as described above (including RNase inhibitor) and organoids (now single cells) were resuspended in OWB buffer containing RNase inhibitor, 2 mM EDTA and 1% RNase-free BSA (Sigma). Cells were passed through a 30 µm cell strainer and single cell FACS sorting performed using the MA900 Sony Sorter. Isolated WβA or non-WβA cells were sorted into 96-well plates containing 4 µl lysis buffer supplemented with 0.1 µl RNase inhibitor (Clonetech), 1.9 µl 0.4% Triton X-100, 1 µl 10 µM 5'-biotinylated oligo-dT30VN (IDT) and 1 µl 10 mM dNTP (Thermo Scientific). Cells were sorted at one cell per well, with bulk controls (10 cells) and empty well controls (0 cells) included for each plate. Plates were snap frozen on dry ice and stored at - 80 ^{0}C for less than 4 weeks.

Single cell cDNA synthesis and library generation were performed according to the SMART-seq2 protocol (Picelli *et al*., 2014), as described (Hu *et al*., 2020). Briefly, cells were lysed by removing plates from - 80 ^{0}C and heating at 72 ^{0}C for 3 min. Plates were then placed at 4 ^{0}C before adding the reverse transcription mix containing 5'-biotinylated TSO (Qiagen). PCR products were cleaned up using 0.8:1 Ampure XP beads (Beckman Coulter) with Biomek FxP Laboratory Automation Workstation (Biomek). Quality of single-cell cDNA was tested using TapeStation, as well as by single cell qPCR for GAPDH or ACTB using the QuantiNova SYBR Green PCR Kit (Qiagen). cDNA concentration was measured using Quant-iT™ PicoGreen™ dsDNA Assay Kit (Invitrogen) on the CLARIOstar Plate Reader (BMG Labtech). Wells with C_T values of GAPDH or ACTB below 20 were selected as wells with a good quality cDNA. Libraries from single cell cDNA were generated using miniaturized Nextera XT (Illumina) protocol (Mora-Castilla *et al*., 2016) with Mosquito HTS (TTP LabTech), in 384-well Endure plate (Life Technology). Library sequencing was performed by Novogene.

Bulk RNA-seq of Wnt/β-catenin signaling reporter organoids

hFT WβS-reporter organoids were generated and dissociated as described above. RNA extraction and DNase digestion were performed using the RNAqueous-Micro Total RNA Isolation Kit (Thermo Fisher Scientific)

according to the manufacturer's protocol. RNA integrity was evaluated using the 2200 TapeStation system (Agilent). The SMARTer Stranded Total RNA-seq kit v2 — Pico Input (Takara) was used to prepare sequencing libraries, which were then assessed with TapeStation (Agilent) and quantified by Qubit (Thermo Fisher Scientific). Library sequencing was performed by Novogene.

Organoid RNA extraction & RT-qPCR

For RNA extraction, organoids were harvested as described above. Pelleted organoids were washed, mechanically fragmented in cold DPBS, pelleted, resuspended in 350 µl RLT buffer (Qiagen) and transferred into a 1.5 ml Eppendorf tube. The tube was incubated for 15 min at room temperature in rotation and then vortexed for 1 min. RNA extraction was performed according to the Qiagen RNeasy Plus Micro Kit. Extracted RNA was tested for concentration (using NanoDrop) and, if required, for quality (using TapeStation). Up to 2 ug of extracted RNA was used to generate cDNA using the High Capacity cDNA Reverse Transcription Kit (Applied Biosystems) or TaqMan™ Reverse Transcription Reagents (Invitrogen). RT-qPCR was set up using the SYBR Green PCR Master Mix (ThermoFisher) and conducted using the StepOnePlus RT-PCR machine (ThermoFisher).

RNA In Situ Hybridization (RNAScope)

A small piece of primary human or mouse tissue was resected and embedded in Fisher Healthcare Tissue-Plus Optimum Cutting Temperature (OCT, ThermoFisher). This was frozen at -80 ^{0}C, sectioned into 10 µm sections using the CryoStar NX50 (Thermo Scientific) cryostat, mounted on regular glass slides (SuperFrost Plus, VWR International) and immediately stored at - 80 ^{0}C. RNA *In situ* Hybridization was performed using the RNAScope® Multiplex Fluorescent v2 kit (ACD) as described (Wang *et al*., 2012) for fresh frozen human or mouse tissue. Organoid sections were derived by dissociating organoids, washing and Cytospining (FisherScientific) to attach dissociated cells on a glass slide. Slides were immediately fixed in 4% PFA. RNA FISH staining was performed as per the RNAScope protocol (ACD).

Organoid Immunofluorescence Staining

Organoids were prepared for antibody staining by culture for 7-12 days on an 8-well microscopy chamber slide (Thistle Scientific). Once ready, whole-mount staining was performed on organoids within Matrigel. Briefly, organoids were washed and fixed for 15-20 min using 2% methanol-free Paraformaldehyde diluted in DPBS (ThermoFisher). To reduce background staining, samples were washed three times (10 min each) with PBS containing 0.4M Glycine (Sigma). Permeabilization was performed for 10 min using 0.5% Triton X-100 in PBS. All washing, blocking and antibody staining steps were performed in wash buffer comprising 0.2% Triton X-100 and 0.05% Tween-20 in PBS. Blocking was done in 5-10% Normal Donkey Serum (Sigma) for 2-3 hrs. Primary antibody incubation was performed overnight at 4 ^{0}C in motion. Secondary antibody incubation was done at 2-3 hrs at room temperature. Samples were mounted in Vectashield Mounting Medium (Vector Laboratories). Images were obtained using the Zeiss LSM 780 Inverted Confocal Microscope.

Cell Culture & Protein Expression / Validation

RSPO1 protein expression and isolation was performed using the HEK293T HA-R-Spondin1-Fc cell line, according to the manufacturer's protocol (Culturex). WNT3A protein expression was performed using the L-WNT3A cell line according to the manufacturer's protocol (ATCC). WNT7A protein was expressed and harvested in HEK293 cells using the pcDNA.Wnt7A construct, a gift from Marian Waterman (Addgene plasmid #35914) and the pcDNA.WNT7A-V5 construct, a gift from Xi He (Addgene plasmid #43816). Other constructs used in this work include pRK5-mFzd3-1D4 (Addgene #42265), pRK5-mFzd5-1D4 (Addgene #42267) and pRK5-mFzd6-1D4 (Addgene #42268), all gifts from Chris Garcia & Jeremy Nathans. All generated proteins, constructs and small molecule inhibitors modulating Wnt signaling were functionally validated with the TOPFlash assay, using the M50 Super 8x TOPFlash (Addgene #12456) and M51 Super 8x FOPFlash (Addgene #12457) constructs, both gifts from Randall Moon (Veeman *et al*., 2003). For hormone-stimulation experiments, pCMV-hERα (Addgene #101141) and pcDNA3-PRβ (Addgene #89130) constructs were used, both gifts from Elizabeth Wilson.

Key Resources / Materials table

REAGENT	SOURCE and IDENTIFIER
CULTURE MEDIUMS AND REAGENTS	
Fetal Bovine Serum, qualified, heat inactivated, E	ThermoFisher (#10500064)
Penicillin Streptomycin (Pen Strep)	ThermoFisher (#15070063)
Lipofectamine 3000 Transfection Reagent	ThermoFisehr (#L3000008)
Lipofectamine RNAiMAX Transfection Reagent	ThermoFisher (#13778030)
Pierce 16% Formaldehyde (w/v)	ThermoFisher (#28908)
Microscope slide, Superfrost plus	VWR (#631-0108)
VECTASHIELD anti-fade mounting medium	Vector Laboratories (#H-1000)
Immedge Hydrophobic Pen	Vector Laboratories (#H-4000)
Dual-Luciferase Reporter Assay System	Promega (#E1910)
Brefeldin A (BFA)	ThermoFisher (#00-4506-51)
Monensin	ThermoFisher (#00-4505-51)
Lambda Protein Phosphatase	New England Biolabs (#P0753S)
PNGase F	New England Biolabs (#P0704S)
Lenti-X Concentrator	Takari Bio (#631231)
Polybrene Reagent	Millipore UK (#TR-1003-G)
Lithium Chloride	Sigma-Aldrich (#203637-10G)
RECOMBINANT PROTEINS & SMALL MOLECULE INHIBITORS	
CHIR99021 (3 µM)	Bio-Techne (#4423/10)
IWP-2 (2 µM)	Bio-Techne (#3533/10)
LGK-974 (2 µM)	Stratech Scientific (#S7143-SEL)

REAGENT	SOURCE and IDENTIFIER
XAV-939 (5 µM)	Stratech Scientific (#S1180-SEL-10 mg)
PRI-724 (10 µM)	Abcam (#ab229168-5mg)
Surrogate Wnt (0.5 nM)	UProtein Express (#N001 - 0.025 mg)
IgG 2919 (FZD5 inhibitor)	Gift from The Sidhu Lab, University of Toronto
IgG 2921 (FZD5 inhibitor)	Gift from The Sidhu Lab, University of Toronto
Wnt3a (conditioned medium)	In-house generated
WNT7A (conditioned medium)	In-house generated
Valproic Acid (1 mM)	Bio-Techne (#2815/100)
DAPT (10 µM)	Bio-Techne (#2634/10)
Estrogen (100 nM)	Bio-Techne (#2824/100)
Progesterone (1 µM)	Bio-Techne (#2835/100)
Wnt3a Protein, human, recombinant	Bio-Techne (#5036-WN-010)
Wnt3a Protein, human, recombinant	AMSbio (#AMS.rhW3aL-002-stab)
Wnt7a Protein, human, recombinant	Abcam (#ab129138)
REAGENTS FOR DISSOCIATION OF PRIMARY TISSUE	
Trypsin from Bovine pancreas	Sigma-Aldrich (#T9935)
Collagenase, Type I	ThermoFisher (#17018029)
Dnase I grade II	Sigma-Aldrich (#000000010104159001)
Red blood Cell Lysis Solution	Miltenyi Biotech (#130-094-183)
ORGANOID CULTURE	
Advanced DMEM/F-12, no phenol red	ThermoFisher (#21041033)
HEPES	ThermoFisher (#15630056)
Penicillin Streptomycin (Pen Strep)	ThermoFisher (#15070063)
Epidermal Growth Factor (EGF), human, recombinant	ThermoFisher (#PHG0311)
Noggin, human, recombinant	Peprotech (#120-10C)
Fibroblast Growth Factor-10 (FGF-10), human, recombinant	Peprotech (#100-26)
Human RSPO1	Peprotech (#120-38-100)
Purified mouse Rspo1	In-house generated
N-2 Supplement	ThermoFisher (#17502048)
B-27 Supplement	ThermoFisher (#12587010)
Nicotinamide	Sigma-Aldrich (#N0636-100G)
N-Acetyl L-Cysteine	Sigma-Aldrich (#A9165-5G)
Forskolin (FSK)	Bio-Techne (#1099/10)
A83.01	Stemcell Technologies (#72022)
Y-27632 (ROCK inhibitor)	Bio-Techne (#1254/10)
Cultrex Organoid Harvesting Solution	Bio-Techne (#3700-100-01)

REAGENT	SOURCE and IDENTIFIER
Matrigel (phenol red-free)	Corning, supplier SLS (#356237)
SINGLE CELL RNA-SEQUENCING	
AMPure XP	Beckman Coulter (#A63881)
KAPA HIFI HotStart ReadyMix PCR kit	Roche Diagnostics (#07958935001)
SuperScript II Reverse Transcriptase	ThermoFisher (#18064071)
Bovine Serum Albumin (BSA, nuclease and protease-free)	Merck Chemicals Ltd (#126609-5GM)
Sequencing generated libraries	Novogene
PROTEIN EXPRESSION AND PURIFICATION	
L Wnt3a cell line	ATCC (#CRL-2647)
HA-R-Spondin1-Fc 293T Cells	AMSbio (#3710-001-01)
CD293 medium	ThermoFisher (#11913019)
GlutaMAX-1 (100X)	ThermoFisher (#35050-061)
RNA EXTRATION AND QPCR	
RNeasy Plus Micro Kit	Qiagen (#74034)
High-Capacity cDNA Reverse Transcription Ki	ThermoFisher (#4368814)
PowerUp SYBR Green Master Mix	ThermoFisher (#A25780)
MicroAmp Fast Optical 96-Well Reaction Plate, 0.1	ThermoFisher (#4346907)
StepOnePlus™ RT PCR System	ThermoFisher (#4376600)
RNA IN SITU HYBRIDIZATION (RNAScope)	
Multiplex Fluorescent Detection Kit v2	Bio-Techne (#323110)
SSC solution (20X)	ThermoFisher (#AM9763)
ACD HybEZ™ II Hybridization System	Bio-Techne (#321720)
Rnase A	Qiagen (#19101)
Probe (3-plex human Positive Control)	Bio-Techne (#320861)
Probe (3-plex mouse Positive Control)	Bio-Techne (#320881)
Probe (3-plex Negative Control)	Bio-Techne (#320871)
Probe (human WNT7A)	Bio-Techne (#408231)
Probe (human AXIN2)	Bio-Techne (#400241-C2)
Probe (human LGR5)	Bio-Techne (#311021-C3)
Probe (mouse Wnt7a)	Bio-Techne (#401121)
Probe (mouse Axin2)	Bio-Techne (#400331-C2)
Probe (mouse Lgr5)	Bio-Techne (#312171-C3)
TSA Plus Fluorescein System	PerkinElmer (#NEL741001KT)
TSA Plus Cyanine 3 System	PerkinElmer (#NEL744001KT)
TSA Plus Cyanine 5 System	PerkinElmer (#NEL745001KT)

ACKNOWLEDGEMENTS

We thank the WIMM FACS core facility, the WIMM Wolfson Imaging Centre and the WIMM Single Cell core facility for their help in this study. This work was supported by Ovarian Cancer Action, the Oxford Biomedical Research Centre, National Institute of Health Research and the Diane Oxberry Trust.

LIST OF REFERENCES

Alexandre, C., Baena-Lopez, A., & Vincent, J.-P. (2013). Patterning and growth control by membrane-tethered Wingless. *Nature 2013 505:7482*, *505*(7482), 180–185. https://doi.org/10.1038/nature12879

Ali, A., Syed, S. M., Jamaluddin, M. F. B., Colino-Sanguino, Y., Gallego-Ortega, D., & Tanwar, P. S. (2020). Cell Lineage Tracing Identifies Hormone-Regulated and Wnt-Responsive Vaginal Epithelial Stem Cells. *Cell Reports*, *30*(5), 1463-1477.e7. https://doi.org/10.1016/j.celrep.2020.01.003

Angers, S. (2021). Wnt signaling inhibition confers induced synthetic lethality to PARP inhibitors. *EMBO Molecular Medicine*, *13*(4), e14002. https://doi.org/10.15252/EMMM.202114002

Barker, N., & Clevers, H. (2010). Leucine-Rich Repeat-Containing G-Protein-Coupled Receptors as Markers of Adult Stem Cells. *Gastroenterology*, Vol. 138, pp. 1681–1696. https://doi.org/10.1053/j.gastro.2010.03.002

Barker, N., Huch, M., Kujala, P., van de Wetering, M., Snippert, H. J., van Es, J. H., … Clevers, H. (2010). Lgr5+ve Stem Cells Drive Self-Renewal in the Stomach and Build Long-Lived Gastric Units In Vitro. *Cell Stem Cell*, *6*(1), 25–36. https://doi.org/10.1016/j.stem.2009.11.013

Bartfeld, S., Bayram, T., Van De Wetering, M., Huch, M., Begthel, H., Kujala, P., … Clevers, H. (2015). In vitro expansion of human gastric epithelial stem cells and their responses to bacterial infection. *Gastroenterology*, *148*(1), 126-136.e6. https://doi.org/10.1053/j.gastro.2014.09.042

Bast, R. C., Klug, T. L., John, E. St., Jenison, E., Niloff, J. M., Lazarus, H., … Knapp, R. C. (1983). A Radioimmunoassay Using a Monoclonal Antibody to Monitor the Course of Epithelial Ovarian Cancer. *New England Journal of Medicine*, *309*(15), 883–887. https://doi.org/10.1056/nejm198310133091503

Björnström, L., & Sjöberg, M. (2005). Mechanisms of Estrogen Receptor Signaling: Convergence of Genomic and Nongenomic Actions on Target Genes. *Molecular Endocrinology*, *19*(4), 833–842. https://doi.org/10.1210/me.2004-0486

Bond, J., Sedmera, D., Jourdan, J., Zhang, Y., Eisenberg, C. A., Eisenberg, L. M., & Gourdie, R. G. (2003). Wnt11 and Wnt7a are up-regulated in association with differentiation of cardiac conduction cells in vitro and in vivo. *Developmental Dynamics*, *227*(4), 536–543. https://doi.org/10.1002/dvdy.10333

Boonekamp, K. E., Heo, I., Artegiani, B., Asra, P., van Son, G., de Ligt, J., & Clevers, H. (2021). Identification of novel human Wnt target genes using adult endodermal tissue-derived organoids. *Developmental Biology*. https://doi.org/10.1016/j.ydbio.2021.01.009

Bui, T. D., Zhang, L., Rees, M. C. P., Bicknell, R., & Harris, A. L. (1997). Expression and hormone regulation of Wnt2, 3, 4, 5a, 7a, 7b and 10b in normal human endometrium and endometrial carcinoma. *British Journal of Cancer*, *75*(8), 1131–1136. https://doi.org/10.1038/bjc.1997.195

Cao, W., Li, M., Liu, J., Zhang, S., Noordam, L., Verstegen, M. M. A., … Pan, Q. (2020). LGR5 marks targetable tumor-initiating cells in mouse liver cancer. *Nature Communications 2020 11:1*, *11*(1), 1–16. https://doi.org/10.1038/s41467-020-15846-0

Carmon, K. S., Gong, X., Lin, Q., Thomas, A., & Liu, Q. (2011). R-spondins function as ligands of the orphan receptors LGR4 and LGR5 to regulate Wnt/β-catenin signaling. *Proceedings of the National Academy of Sciences of the United States of America*, *108*(28), 11452–11457. https://doi.org/10.1073/pnas.1106083108

Chen, F., Gaitskell, K., Garcia, M., Albukhari, A., Tsaltas, J., & Ahmed, A. (2017). Serous tubal intraepithelial carcinomas associated with high-grade serous ovarian carcinomas: a systematic review. *BJOG: An International Journal of Obstetrics & Gynaecology*, *124*(6), 872–878. https://doi.org/10.1111/1471-0528.14543

Clevers, H. (2006). Wnt/β-Catenin Signaling in Development and Disease. *Cell*, *127*(3), 469–480. https://doi.org/10.1016/J.CELL.2006.10.018

Clevers, H., Loh, K. M., & Nusse, R. (2014). An integral program for tissue renewal and regeneration: Wnt signaling and stem cell control. *Science*, *346*(6205). https://doi.org/10.1126/SCIENCE.1248012/ASSET/2B86C789-E77F-4290-AF68-B234AA81AFD5/ASSETS/GRAPHIC/346_1248012_F4.JPEG

Couse, J. F., Dixon, D., Yates, M., Moore, A. B., Ma, L., Maas, R., & Korach, K. S. (2001). Estrogen receptor-α knockout mice exhibit resistance to the developmental effects of neonatal diethylstilbestrol exposure on the female reproductive tract. *Developmental Biology*, *238*(2), 224–238. https://doi.org/10.1006/dbio.2001.0413

Crum, C. P. (2009, April). Intercepting pelvic cancer in the distal fallopian tube: Theories and realities. *Molecular Oncology*, Vol. 3, pp. 165–170. https://doi.org/10.1016/j.molonc.2009.01.004

de Lau, W., Barker, N., Low, T. Y., Koo, B.-K., Li, V. S. W., Teunissen, H., … Clevers, H. (2011). Lgr5 homologues associate with Wnt receptors and mediate R-spondin signalling. *Nature*, *476*(7360), 293–297. https://doi.org/10.1038/nature10337

de Witte, C. J., Espejo Valle-Inclan, J., Hami, N., Lõhmussaar, K., Kopper, O., Vreuls, C. P. H., … Stelloo, E. (2020). Patient-Derived Ovarian Cancer Organoids Mimic Clinical Response and Exhibit Heterogeneous Inter- and Intrapatient Drug Responses. *Cell Reports*, *31*(11), 107762. https://doi.org/10.1016/j.celrep.2020.107762

DeCherney, A. H., Cholst, I., & Naftolin, F. (1981). Structure and function of the fallopian tubes following exposure to diethylstilbestrol (DES) during gestation. *Fertility and Sterility*, *36*(6), 741–745. https://doi.org/10.1016/S0015-0282(16)45919-4

Dinh, H. Q., Lin, X., Abbasi, F., Nameki, R., Haro, M., Olingy, C. E., … Lawrenson, K. (2021). Single-cell transcriptomics identifies gene expression networks driving differentiation and tumorigenesis in the human fallopian tube. *Cell Reports*, *35*(2), 108978. https://doi.org/10.1016/j.celrep.2021.108978

Dong, B., Vold, S., Olvera-Jaramillo, C., & Chang, H. (2018). Functional redundancy of frizzled 3 and frizzled 6 in planar cell polarity control of mouse hair follicles. *Development (Cambridge)*, *145*(19). https://doi.org/10.1242/dev.168468

Dunlap, K. A., Filant, J., Hayashi, K., Rucker, E. B., Song, G., Deng, J. M., … Spencer, T. E. (2011). Postnatal Deletion of Wnt7a Inhibits Uterine Gland Morphogenesis and Compromises Adult Fertility in Mice1. *Biology of Reproduction*, *85*(2), 386–396. https://doi.org/10.1095/biolreprod.111.091769

Erickson, B. K., Conner, M. G., & Landen, C. N. (2013). The role of the fallopian tube in the origin of ovarian cancer. *American Journal of Obstetrics and Gynecology*, Vol. 209, pp. 409–414. https://doi.org/10.1016/j.ajog.2013.04.019

Farin, H. F., Jordens, I., Mosa, M. H., Basak, O., Korving, J., Tauriello, D. V. F., … Clevers, H. (2016). Visualization of a short-range Wnt gradient in the intestinal stem-cell niche. *Nature*, *530*(7590), 340–343. https://doi.org/10.1038/nature16937

Finch, A., Shaw, P., Rosen, B., Murphy, J., Narod, S. A., & Colgan, T. J. (2006). Clinical and pathologic findings of prophylactic salpingo-oophorectomies in 159 BRCA1 and BRCA2 carriers. *Gynecologic Oncology*, *100*(1), 58–64. https://doi.org/10.1016/j.ygyno.2005.06.065

Ghorpade, D. S., Ozcan, L., Zheng, Z., Nicoloro, S. M., Shen, Y., Chen, E., … Tabas, I. (2018). Hepatocyte-secreted DPP4 in obesity promotes adipose inflammation and insulin resistance. *Nature*, *555*(7698), 673–677. https://doi.org/10.1038/nature26138

Ghosh, A., Syed, S. M., & Tanwar, P. S. (2017). *In vivo genetic cell lineage tracing reveals that oviductal secretory cells self-renew and give rise to ciliated cells*. https://doi.org/10.1242/dev.149989

Glinka, A., Dolde, C., Kirsch, N., Huang, Y. L., Kazanskaya, O., Ingelfinger, D., … Niehrs, C. (2011). LGR4 and LGR5 are R-spondin receptors mediating Wnt/β-catenin and Wnt/PCP signalling. *EMBO Reports*, *12*(10), 1055–1061. https://doi.org/10.1038/embor.2011.175

Goldstein, B., Takeshita, H., Mizumoto, K., & Sawa, H. (2006). Wnt signals can function as positional cues in establishing cell polarity. *Developmental Cell*, *10*(3), 391–396. https://doi.org/10.1016/j.devcel.2005.12.016

Gunin, A. G., Emelianov, V. U., Mironkin, I. U., Morozov, M. P., & Tolmachev, A. S. (2004). Lithium treatment enhances estradiol-induced proliferation and hyperplasia formation in the uterus of mice. *European Journal of Obstetrics and Gynecology and Reproductive Biology*, *114*(1), 83–91. https://doi.org/10.1016/j.ejogrb.2003.09.023

Hall, A. C., Lucas, F. R., & Salinas, P. C. (2000). Axonal remodeling and synaptic differentiation in the cerebellum is regulated by WNT-7a signaling. *Cell*, *100*(5), 525–535. https://doi.org/10.1016/S0092-8674(00)80689-3

Hao, H. X., Xie, Y., Zhang, Y., Zhang, O., Oster, E., Avello, M., … Cong, F. (2012). ZNRF3 promotes Wnt receptor turnover in an R-spondin-sensitive manner. *Nature*, *485*(7397), 195–202. https://doi.org/10.1038/nature11019

He, F., Xiong, W., Yu, X., Espinoza-Lewis, R., Liu, C., Gu, S., … Chen, Y. P. (2008). Wnt5a regulates directional cell migration and cell proliferation via Ror2-mediated noncanonical pathway in mammalian palate development. *Development*, *135*(23), 3871–3879. https://doi.org/10.1242/dev.025767

Hideyuki, N., Saito, T., Yamasaki, H., Mizumoto, H., Ito, E., & Kudo, R. (1999). Nuclear localization of β-catenin in normal and carcinogenic endometrium. *Molecular Carcinogenesis*, *25*(3), 207–218. https://doi.org/10.1002/(SICI)1098-2744(199907)25:3<207::AID-MC7>3.0.CO;2-4

Hill, S. J., Decker, B., Roberts, E. A., Horowitz, N. S., Muto, M. G., Worley, M. J., … D'Andrea, A. D. (2018). Prediction of DNA repair inhibitor response in short-term patient-derived ovarian cancer organoids. *Cancer Discovery*, *8*(11), 1404–1421. https://doi.org/10.1158/2159-8290.CD-18-0474

Hoffmann, K., Berger, H., Kulbe, H., Thillainadarasan, S., Mollenkopf, H., Zemojtel, T., … Kessler, M. (2020). Stable expansion of high-grade serous ovarian cancer organoids requires a low-Wnt environment. *The EMBO Journal*, *e104013*, 1–23. https://doi.org/10.15252/embj.2019104013

Hou, Y. F., Yuan, S. T., Li, H. C., Wu, J., Lu, J. S., Liu, G., … Shao, Z. M. (2004). ERβ exerts multiple stimulative effects on human breast carcinoma cells.

Oncogene, *23*(34), 5799–5806. https://doi.org/10.1038/sj.onc.1207765

Howitt, B. E., Hanamornroongruang, S., Lin, D. I., Conner, J. E., Schulte, S., Horowitz, N., … Meserve, E. E. (2015). Evidence for a Dualistic Model of High-grade Serous Carcinoma. *The American Journal of Surgical Pathology*, *39*(3), 287–293. https://doi.org/10.1097/PAS.0000000000000369

Hu, Z., Artibani, M., Alsaadi, A., Wietek, N., Morotti, M., Shi, T., … Ahmed, A. A. (2020). The Repertoire of Serous Ovarian Cancer Non-genetic Heterogeneity Revealed by Single-Cell Sequencing of Normal Fallopian Tube Epithelial Cells. *Cancer Cell*, *37*(2), 226-242.e7. https://doi.org/10.1016/j.ccell.2020.01.003

Huang, S. M. A., Mishina, Y. M., Liu, S., Cheung, A., Stegmeier, F., Michaud, G. A., … Cong, F. (2009). Tankyrase inhibition stabilizes axin and antagonizes Wnt signalling. *Nature*, *461*(7264), 614–620. https://doi.org/10.1038/nature08356

Huch, M., Bonfanti, P., Boj, S. F., Sato, T., Loomans, C. J. M., van de Wetering, M., … Clevers, H. (2013). Unlimited in vitro expansion of adult bi-potent pancreas progenitors through the Lgr5/R-spondin axis. *The EMBO Journal*, *32*(20), 2708–2721. https://doi.org/10.1038/emboj.2013.204

Huch, M., Dorrell, C., Boj, S. F., Van Es, J. H., Li, V. S. W., Van De Wetering, M., … Clevers, H. (2013). In vitro expansion of single Lgr5 + liver stem cells induced by Wnt-driven regeneration. *Nature*, *494*(7436), 247–250. https://doi.org/10.1038/nature11826

Huch, M., Gehart, H., van Boxtel, R., Hamer, K., Blokzijl, F., Verstegen, M. M. A., … Clevers, H. (2015). Long-term culture of genome-stable bipotent stem cells from adult human liver. *Cell*, *160*(1–2), 299–312. https://doi.org/10.1016/j.cell.2014.11.050

Hwang, S. G., Ryu, J. H., Kim, I. C., Jho, E. H., Jung, H. C., Kim, K., … Chun, J. S. (2004). Wnt-7a causes loss of differentiated phenotype and inhibits apoptosis of articular chondrocytes via different mechanisms. *Journal of Biological Chemistry*, *279*(25), 26597–26604. https://doi.org/10.1074/jbc.M401401200

Ingaramo, P. I., Milesi, M. M., Schimpf, M. G., Ramos, J. G., Vigezzi, L., Muñoz-de-Toro, M., … Varayoud, J. (2016). Endosulfan affects uterine development and functional differentiation by disrupting Wnt7a and β-catenin expression in rats. *Molecular and Cellular Endocrinology*, *425*, 37–47. https://doi.org/10.1016/j.mce.2016.02.011

Janda, C. Y., Dang, L. T., You, C., Chang, J., Lau, W. De, Zhong, Z. A., … Garcia, K. C. (2017). Surrogate Wnt agonists that phenocopy canonical Wnt and β-catenin signalling. *Nature*, *545*(7653), 234–237. https://doi.org/10.1038/nature22306

Karthaus, W. R., Iaquinta, P. J., Drost, J., Gracanin, A., Van Boxtel, R., Wongvipat, J., … Clevers, H. C. (2014). Identification of multipotent luminal progenitor cells in human prostate organoid cultures. *Cell*, *159*(1), 163–175. https://doi.org/10.1016/j.cell.2014.08.017

Kaur, A., Lim, J. Y. S., Sepramaniam, S., Patnaik, S., Harmston, N., Lee, M. A., … Madan, B. (2021). WNT inhibition creates a BRCA-like state in Wnt-addicted cancer. *EMBO Molecular Medicine*, *13*(4). https://doi.org/10.15252/EMMM.202013349

Kessler, M., Hoffmann, K., Brinkmann, V., Thieck, O., Jackisch, S., Toelle, B., … Meyer, T. F. (2015). The Notch and Wnt pathways regulate stemness and differentiation in human fallopian tube organoids. *Nature Communications*, *6*(May), 8989. https://doi.org/10.1038/ncomms9989

Kessler, M., Hoffmann, K., Fritsche, K., Brinkmann, V., Mollenkopf, H.-J., Thieck, O., … Meyer, T. F. (2019). Chronic Chlamydia infection in human organoids increases stemness and promotes age-dependent CpG methylation. *Nature Communications*, *10*(1), 1194. https://doi.org/10.1038/s41467-019-09144-7

Kim, J., Park, E. Y., Kim, O., Schilder, J. M., Coffey, D. M., Cho, C. H., & Bast, R. C. (2018, November 12). Cell origins of high-grade serous ovarian cancer. *Cancers*, Vol. 10. https://doi.org/10.3390/cancers10110433

King, M. L., Lindberg, M. E., Stodden, G. R., Okuda, H., Ebers, S. D., Johnson, A., … Hayashi, K. (2015). WNT7A/β-catenin signaling induces FGF1 and influences sensitivity to niclosamide in ovarian cancer. *Oncogene*, *34*(26), 3452–3462. https://doi.org/10.1038/onc.2014.277

Kopper, O., de Witte, C. J., Lõhmussaar, K., Valle-Inclan, J. E., Hami, N., Kester, L., … Clevers, H. (2019). An organoid platform for ovarian cancer captures intra- and interpatient heterogeneity. *Nature Medicine*, 1. https://doi.org/10.1038/s41591-019-0422-6

Kouzmenko, A. P., Takeyama, K. I., Ito, S., Furutani, T., Sawatsubashi, S., Maki, A., … Kato, S. (2004). Wnt/β-catenin and estrogen signaling converge in vivo. *Journal of Biological Chemistry*, *279*(39), 40255–40258. https://doi.org/10.1074/jbc.C400331200

Kroeger, P. T., & Drapkin, R. (2017). Pathogenesis and heterogeneity of ovarian cancer. *Current Opinion in Obstetrics and Gynecology*, *29*(1), 26–34. https://doi.org/10.1097/GCO.0000000000000340

Kuhn, E., Kurman, R. J., Vang, R., Sehdev, A. S., Han, G., Soslow, R., … Shih, I.-M. (2012). TP53 mutations in serous tubal intraepithelial carcinoma and concurrent pelvic high-grade serous carcinoma-evidence supporting the clonal relationship of the two lesions. *The Journal of Pathology*, *226*(3), 421–426. https://doi.org/10.1002/path.3023

Labidi-Galy, S. I., Papp, E., Hallberg, D., Niknafs, N., Adleff, V., Noe, M., … Velculescu, V. E. (2017). High grade serous ovarian carcinomas originate in the fallopian tube. *Nature Communications*, *8*(1), 1093. https://doi.org/10.1038/s41467-017-00962-1

Leushacke, M., Tan, S. H., Wong, A., Swathi, Y., Hajamohideen, A., Tan, L. T., … Barker, N. (2017). Lgr5-expressing chief cells drive epithelial regeneration and cancer in the oxyntic stomach. *Nature Cell Biology*, *19*(7), 774–786. https://doi.org/10.1038/ncb3541

Lõhmussaar, K., Kopper, O., Korving, J., Begthel, H., Vreuls, C. P. H., van Es, J. H., & Clevers, H. (2020). Assessing the origin of high-grade serous ovarian cancer using CRISPR-modification of mouse organoids. *Nature Communications*, *11*(1), 2660. https://doi.org/10.1038/s41467-020-16432-0

McLachlan, J. A., Newbold, R. R., & Bullock, B. C. (1980). Long-Term Effects on the Female Mouse Genital Tract Associated with Prenatal Exposure to Diethylstilbestrol. *Cancer Research*, *40*(11).

Mericskay, M., Kitajewski, J., & Sassoon, D. (2004). Wnt5a is required for proper epithelial-mesenchymal interactions in the uterus. *Development*, *131*(9), 2061–2072. https://doi.org/10.1242/dev.01090

Miller, C., Degenhardt, K., & Sassoon, D. A. (1998). Fetal exposure to DES results in de-regulation of Wnt7a during uterine morphogenesis [2]. *Nature Genetics*, Vol. 20, pp. 228–230. https://doi.org/10.1038/3027

Miller, C., & Sassoon, D. A. (1998). Wnt-7a maintains appropriate uterine patterning during the development of the mouse female reproductive tract. *Development*, *125*(16).

Miller, Cary, Pavlova, A., & Sassoon, D. A. (1998). Differential expression patterns of Wnt genes in the murine female reproductive tract during development and the estrous cycle. *Mechanisms of Development*, *76*(1–2), 91–99. https://doi.org/10.1016/S0925-4773(98)00112-9

Ng, A., Tan, S., Singh, G., Rizk, P., Swathi, Y., Tan, T. Z., … Barker, N. (2014). Lgr5 marks stem/progenitor cells in ovary and tubal epithelia. *Nature Cell Biology*, *16*(8), 745–757. https://doi.org/10.1038/ncb3000

Okazaki, H., Sato, S., Koyama, K., Morizumi, S., Abe, S., Azuma, M., … Nishioka, Y. (2019). The novel inhibitor PRI-724 for Wnt/β-catenin/CBP signaling ameliorates bleomycin-induced pulmonary fibrosis in mice. *Experimental Lung Research*, *45*(7), 188–199. https://doi.org/10.1080/01902148.2019.1638466

Olson, D. J., & Gibo, D. M. (1998). Antisense wnt-5a mimics wnt-1-mediated C57MG mammary epithelial cell transformation. *Experimental Cell Research*, *241*(1), 134–141. https://doi.org/10.1006/excr.1998.4030

Paik, D. Y., Janzen, D. M., Schafenacker, A. M., Velasco, V. S., Shung, M. S., Cheng, D., … Memarzadeh, S. (2012). Stem-Like Epithelial Cells Are Concentrated in the Distal End of the Fallopian Tube: A Site for Injury and Serous Cancer Initiation. *STEM CELLS*, *30*(11), 2487–2497. https://doi.org/10.1002/stem.1207

Park, S., Cui, J., Yu, W., Wu, L., Carmon, K. S., & Liu, Q. J. (2018). Differential activities and mechanisms of the four r-spondins in potentiating wnt/-catenin signaling. *Journal of Biological Chemistry*, *293*(25), 9759–9769. https://doi.org/10.1074/JBC.RA118.002743/ATTACHMENT/7D21F42A-0024-4AE9-A571-DB0E05669870/MMC1.PDF

Parr, B. A., & McMahon, A. P. (1998). Sexually dimorphic development of the mammalian reproductive tract requires Wnt-7a. *Nature*, *395*(6703), 707–710. https://doi.org/10.1038/27221

Partridge, E., Kreimer, A. R., Greenlee, R. T., Williams, C., Xu, J. L., Church, T. R., … Buys, S. S. (2009). Results from four rounds of ovarian cancer screening in a randomized trial. *Obstetrics and Gynecology*, *113*(4), 775–782. https://doi.org/10.1097/AOG.0b013e31819cda77

Picelli, S., Faridani, O. R., Björklund, Å. K., Winberg, G., Sagasser, S., & Sandberg, R. (2014). Full-length RNA-seq from single cells using Smart-seq2. *Nature Protocols*, *9*(1), 171–181. https://doi.org/10.1038/nprot.2014.006

Polotsky, A. J., Zhu, L., Santoro, N., & Pollard, J. W. (2009). Lithium chloride treatment induces epithelial cell proliferation in xenografted human endometrium. *Human Reproduction*, *24*(8), 1960–1967. https://doi.org/10.1093/humrep/dep115

Qian, D., Jones, C., Rzadzinska, A., Mark, S., Zhang, X., Steel, K. P., … Chen, P. (2007). Wnt5a functions in planar cell polarity regulation in mice. *Developmental Biology*, *306*(1), 121–133. https://doi.org/10.1016/j.ydbio.2007.03.011

Rangel, L. B. A., Agarwal, R., D'Souza, T., Pizer, E. S., Alò, P. L., Lancaster, W. D., … Morin, P. J. (2003). Tight Junction Proteins Claudin-3 and Claudin-4 Are Frequently Overexpressed in Ovarian Cancer but Not in Ovarian Cystadenomas. *Clinical Cancer Research*, *9*(7).

Röhrborn, D., Wronkowitz, N., & Eckel, J. (2015). DPP4 in diabetes. *Frontiers in Immunology*, Vol. 6. https://doi.org/10.3389/fimmu.2015.00386

Rosen, D. G., Wang, L., Atkinson, J. N., Yu, Y., Lu, K. H., Diamandis, E. P., … Bast, R. C. (2005). Potential markers that complement expression of CA125 in epithelial ovarian cancer. *Gynecologic Oncology*, *99*(2), 267–277. https://doi.org/10.1016/j.ygyno.2005.06.040

Sakaki-Yumoto, M., Katsuno, Y., & Derynck, R. (2013, February). TGF-β family signaling in stem cells. *Biochimica et Biophysica Acta - General Subjects*, Vol. 1830, pp. 2280–2296. https://doi.org/10.1016/j.bbagen.2012.08.008

Sato, T., van Es, J. H., Snippert, H. J., Stange, D. E., Vries, R. G., van den Born, M., … Clevers, H. (2011). Paneth cells constitute the niche for Lgr5 stem cells in intestinal crypts. *Nature*, *469*(7330), 415–418. https://doi.org/10.1038/nature09637

Sato, T., Vries, R. G., Snippert, H. J., Van De Wetering, M., Barker, N., Stange, D. E., … Clevers, H. (2009). Single Lgr5 stem cells build crypt-villus structures in vitro without a mesenchymal niche. *Nature*, *459*(7244), 262–265. https://doi.org/10.1038/nature07935

Seishima, R., Leung, C., Yada, S., Murad, K. B. A., Tan, L. T., Hajamohideen, A., … Barker, N. (2019). Neonatal Wnt-dependent Lgr5 positive stem cells are essential for uterine gland development. *Nature Communications*, *10*(1). https://doi.org/10.1038/s41467-019-13363-3

Serra, D., Mayr, U., Boni, A., Lukonin, I., Rempfler, M., Meylan, L. C., … Liberali, P. (2019). Self-organization and symmetry breaking in intestinal organoid

development. *Nature*, *569*(7754), 66. https://doi.org/10.1038/S41586-019-1146-Y

Sigal, M., Logan, C. Y., Kapalczynska, M., Mollenkopf, H. J., Berger, H., Wiedenmann, B., … Meyer, T. F. (2017). Stromal R-spondin orchestrates gastric epithelial stem cells and gland homeostasis. *Nature*, *548*(7668), 451–455. https://doi.org/10.1038/nature23642

Snegovskikh, V., Mutlu, L., Massasa, E., & Taylor, H. S. (2014). Identification of putative fallopian tube stem cells. *Reproductive Sciences*, *21*(12), 1460–1464. https://doi.org/10.1177/1933719114553448

Stange, D. E., Koo, B. K., Huch, M., Sibbel, G., Basak, O., Lyubimova, A., … Clevers, H. (2013). Differentiated Troy+ chief cells act as reserve stem cells to generate all lineages of the stomach epithelium. *Cell*, *155*(2), 357. https://doi.org/10.1016/j.cell.2013.09.008

Steinhart, Z., Pavlovic, Z., Chandrashekhar, M., Hart, T., Wang, X., Zhang, X., … Angers, S. (2017). Genome-wide CRISPR screens reveal a Wnt–FZD5 signaling circuit as a druggable vulnerability of RNF43-mutant pancreatic tumors. *Nature Medicine*, *23*(1), 60–68. https://doi.org/10.1038/nm.4219

Syed, S. M., Kumar, M., Ghosh, A., Tomasetig, F., Ali, A., Whan, R. M., … Tanwar, P. S. (2020). Endometrial Axin2+ Cells Drive Epithelial Homeostasis, Regeneration, and Cancer following Oncogenic Transformation. *Cell Stem Cell*, *26*(1), 64-80.e13. https://doi.org/10.1016/j.stem.2019.11.012

Tojo, M., Hamashima, Y., Hanyu, A., Kajimoto, T., Saitoh, M., Miyazono, K., … Imamura, T. (2005). The ALK-5 inhibitor A-83-01 inhibits Smad signaling and epithelial-to-mesenchymal transition by transforming growth factor-beta. *Cancer Science*, *96*(11), 791–800. https://doi.org/10.1111/j.1349-7006.2005.00103.x

Topol, L., Jiang, X., Choi, H., Garrett-Beal, L., Carolan, P. J., & Yang, Y. (2003). Wnt-5a inhibits the canonical Wnt pathway by promoting GSK-3-independent β-catenin degradation. *Journal of Cell Biology*, *162*(5), 899–908. https://doi.org/10.1083/jcb.200303158

Turco, M. Y., Gardner, L., Hughes, J., Cindrova-Davies, T., Gomez, M. J., Farrell, L., … Burton, G. J. (2017). Long-term, hormone-responsive organoid cultures of human endometrium in a chemically defined medium. *Nature Cell Biology*, *19*(5), 568–577. https://doi.org/10.1038/ncb3516

Tüysüz, N., van Bloois, L., van den Brink, S., Begthel, H., Verstegen, M. M. A., Cruz, L. J., … ten Berge, D. (2017). Lipid-mediated Wnt protein stabilization enables serum-free culture of human organ stem cells. *Nature Communications*, *8*, 14578. https://doi.org/10.1038/ncomms14578

Van Camp, J. K., Beckers, S., Zegers, D., & Van Hul, W. (2014). Wnt Signaling and the Control of Human Stem Cell Fate. *Stem Cell Reviews and Reports*, *10*(2), 207–229. https://doi.org/10.1007/S12015-013-9486-8/FIGURES/3

van den Heuvel, M., Nusse, R., Johnston, P., & Lawrence, P. A. (1989). Distribution of the wingless gene product in drosophila embryos: A protein involved in cell-cell communication. *Cell*, *59*(4), 739–749. https://doi.org/10.1016/0092-8674(89)90020-2

Voloshanenko, O., Gmach, P., Winter, J., Kranz, D., & Boutros, M. (2017). Mapping of Wnt-Frizzled interactions by multiplex CRISPR targeting of receptor gene families. *The FASEB Journal*, *31*(11), 4832–4844. https://doi.org/10.1096/fj.201700144R

Wagner, J., & Lehmann, L. (2006). Estrogens modulate the gene expression of Wnt-7a in cultured endometrial adenocarcinoma cells. *Molecular*
http://www.ncbi.nlm.nih.gov/pubmed/20845993

Zhu, M., Iwano, T., & Takeda, S. (2020). Fallopian tube basal stem cells reproducing the epithelial sheets in vitro—stem cell of fallopian epithelium. *Biomolecules*, *10*(9), 1–15. https://doi.org/10.3390/biom10091270

Nutrition and Food Research, *50*(4–5), 368–372. https://doi.org/10.1002/mnfr.200500215

Wang, B., Zhao, L., Fish, M., Logan, C. Y., & Nusse, R. (2015). Self-renewing diploid Axin2 + cells fuel homeostatic renewal of the liver. *Nature*, *524*(7564), 180–185. https://doi.org/10.1038/nature14863

Wang, Y., Sacchetti, A., Dijk, M. R. van, Zee, M. van der, Horst, P. H. van der, Joosten, R., … Fodde, R. (2012). Identification of Quiescent, Stem-Like Cells in the Distal Female Reproductive Tract. *PLoS ONE*, *7*(7), e40691. https://doi.org/10.1371/JOURNAL.PONE.0040691

Worley, B. L., Kim, Y. S., Mardini, J., Zaman, R., Leon, K. E., Vallur, P. G., … Hempel, N. (2019). GPx3 supports ovarian cancer progression by manipulating the extracellular redox environment. *Redox Biology*, *25*. https://doi.org/10.1016/j.redox.2018.11.009

Xie, Y., Park, E.-S., Xiang, D., & Li, Z. (2018). Long-term organoid culture reveals enrichment of organoid-forming epithelial cells in the fimbrial portion of mouse fallopian tube. *Stem Cell Research*, *32*, 51–60. https://doi.org/10.1016/J.SCR.2018.08.021

Yamamoto, Y., Ning, G., Howitt, B. E., Mehra, K., Wu, L., Wang, X., … Xian, W. (2016). *In vitro* and *in vivo* correlates of physiological and neoplastic human Fallopian tube stem cells. *The Journal of Pathology*, *238*(4), 519–530. https://doi.org/10.1002/path.4649

Yin, X., Farin, H. F., van Es, J. H., Clevers, H., Langer, R., & Karp, J. M. (2013). Niche-independent high-purity cultures of Lgr5+ intestinal stem cells and their progeny. *Nature Methods*, *11*(1), 106–112. https://doi.org/10.1038/nmeth.2737

Yoshioka, S., King, M. L., Ran, S., Okuda, H., MacLean, J. A., McAsey, M. E., … Hayashi, K. (2012). WNT7A Regulates Tumor Growth and Progression in Ovarian Cancer through the WNT/ -Catenin Pathway. *Molecular Cancer Research*, *10*(3), 469–482. https://doi.org/10.1158/1541-7786.MCR-11-0177

You, Y., Huang, T., Richer, E. J., Schmidt, J. E. H., Zabner, J., Borok, Z., & Brody, S. L. (2004). Role of f-box factor foxj1 in differentiation of ciliated airway epithelial cells. *American Journal of Physiology - Lung Cellular and Molecular Physiology*, *286*(4 30-4). https://doi.org/10.1152/ajplung.00170.2003

Yu, H., Ye, X., Guo, N., & Nathans, J. (2012). Frizzled 2 and frizzled 7 function redundantly in convergent extension and closure of the ventricular septum and palate: evidence for a network of interacting genes. *Development (Cambridge, England)*, *139*(23), 4383–4394. https://doi.org/10.1242/dev.083352

Yu, X., Ng, C. P., Habacher, H., & Roy, S. (2008). Foxj1 transcription factors are master regulators of the motile ciliogenic program. *Nature Genetics*, *40*(12), 1445–1453. https://doi.org/10.1038/ng.263

Zhang, S., Dolgalev, I., Zhang, T., Ran, H., Levine, D. A., & Neel, B. G. (2019). Both fallopian tube and ovarian surface epithelium are cells-of-origin for high-grade serous ovarian carcinoma. *Nature Communications*, *10*(1), 5367. https://doi.org/10.1038/s41467-019-13116-2

Zhang, X. L., Peng, C. J., Peng, J., Jiang, L. Y., Ning, X. M., & Zheng, J. H. (2010). Prognostic role of Wnt7a expression in ovarian carcinoma patients. *Neoplasma*, *57*(6), 545–551. Retrieved from

Single Cell Transcriptomics identifies a WNT7A-FZD5 Signaling Axis that maintains Fallopian Tube Stem Cells in Patient-derived Organoids

Abdulkhaliq Alsaadi [1,2,a], Mara Artibani [1,2,3], Zhiyuan Hu [1,2,3], Nina Wietek [1,2,4], Matteo Morotti [1,2,4,b], Laura Santana Gonzales [1,2], Moiad Alazzam [4], Jason Jiang [4], Beena Abdul [4], Hooman Soleymani majd[5], Levi L Blazer [6], Jarret Adams [6], Sachdev S Sidhu [6,7], Joan S. Brugge [8,9] and Ahmed Ashour Ahmed [1,2,4,*]

1 Ovarian Cancer Cell Laboratory, MRC Weatherall Institute of Molecular Medicine, University of Oxford, Oxford OX3 9DS, UK.
2 Nuffield Department of Women's & Reproductive Health, University of Oxford, Oxford OX3 9DU, UK.
3 Gene Regulatory Networks in Development and Disease Laboratory, MRC Weatherall Institute of Molecular Medicine, Radcliffe Department of Medicine, University of Oxford, Oxford OX3 9DS, UK.
4 Department of Gynaecological Oncology, Churchill Hospital, Oxford University Hospitals, Oxford OX3 7LE, UK.
5 Medical Sciences Division, University of Oxford, John Radcliffe Hospital, Oxford OX3 9DU, UK.
6 Donnelly Centre for Cellular and Biomolecular Research, Banting and Best Department of Medical Research, University of Toronto, Toronto, Toronto, Ontario M5S3E1, Canada.
7 Department of Molecular Genetics, University of Toronto, Toronto, Ontario M5S 1A8, Canada.
8 Department of Cell Biology, Harvard Medical School, Boston, MA 02115, USA.
9 Ludwig Center at Harvard, Boston, MA, USA.

[a] Present address: Department of Cell Biology, Harvard Medical School, Boston, MA 02115, USA (abdulkhaliq_alsaadi@hms.harvard.edu)
[b] Present address: Ludwig Institute for Cancer Research, University Hospital of Lausanne (CHUV), Lausanne, Switzerland
* Correspondence: ahmed.ahmed@wrh.ox.ac.uk

MAIN FIGURES

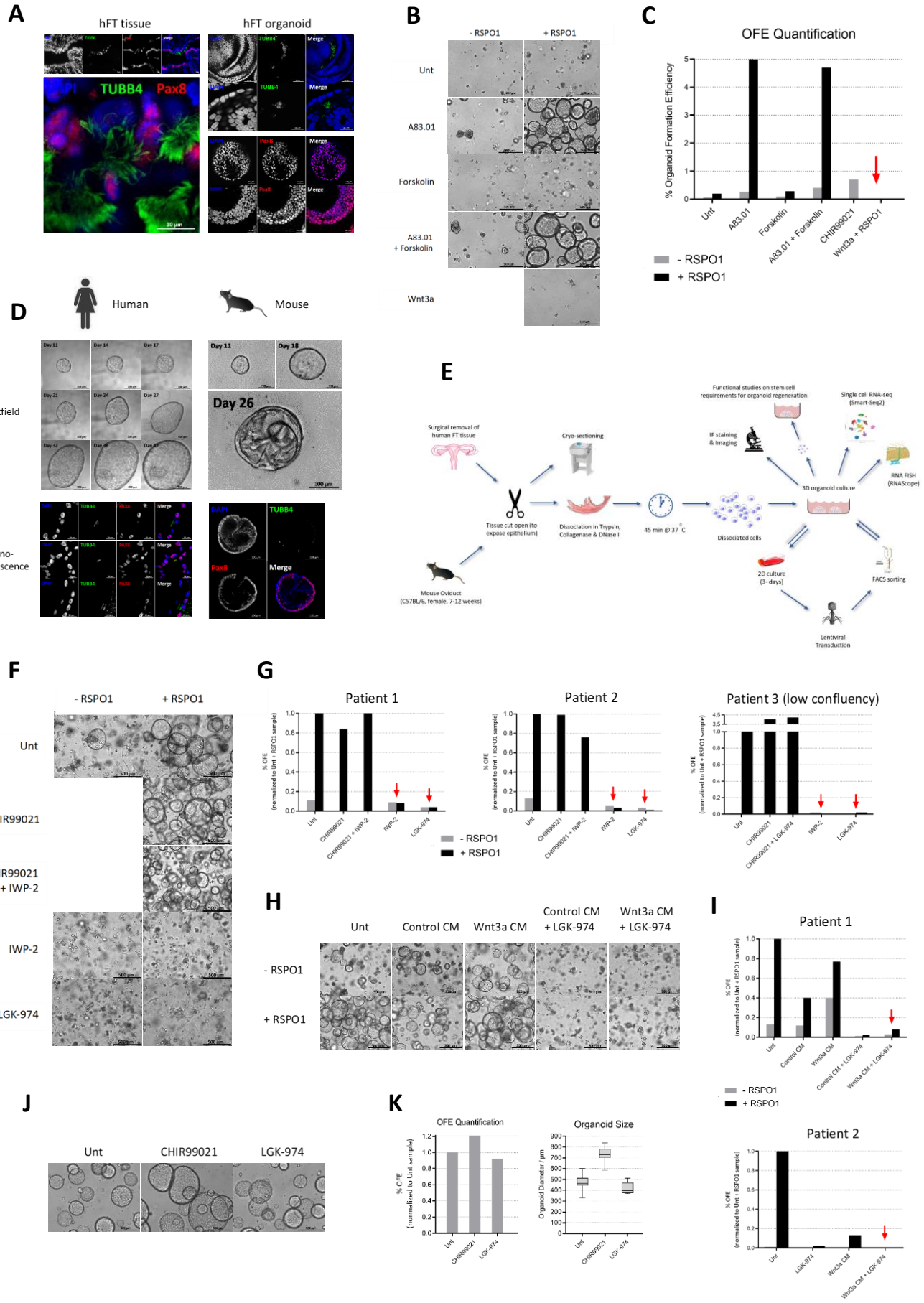
A
hFT tissue
hFT organoid
DAPI
TUBB4
Pax8
Merge
B
- RSPO1
+ RSPO1
Unt
A83.01
Forskolin
A83.01 + Forskolin
Wnt3a
C
OFE Quantification
% Organoid Formation Efficiency
Unt
A83.01
Forskolin
A83.01 + Forskolin
CHIR99021
Wnt3a + RSPO1
- RSPO1
+ RSPO1
D
Human
Mouse
Brightfield
Immuno-fluorescence
Day 26
E
Surgical removal of human FT tissue
Cryo-sectioning
Tissue cut open (to expose epithelium)
Dissociation in Trypsin, Collagenase & DNase I
45 min @ 37 °C
Dissociated cells
3D organoid culture
Functional studies on stem cell requirements for organoid regeneration
Single cell RNA-seq (Smart-Seq2)
IF staining & imaging
RNA FISH (RNAScope)
2D culture (3- days)
FACS sorting
Lentiviral Transduction
Mouse Oviduct (C57BL/6, female, 7-12 weeks)
F
- RSPO1
+ RSPO1
Unt
CHIR99021
CHIR99021 + IWP-2
IWP-2
LGK-974
G
Patient 1
Patient 2
Patient 3 (low confluency)
% OFE (normalized to Unt + RSPO1 sample)
Unt
CHIR99021
CHIR99021 + IWP-2
IWP-2
LGK-974
CHIR99021 + LGK-974
- RSPO1
+ RSPO1
H
Unt
Control CM
Wnt3a CM
Control CM + LGK-974
Wnt3a CM + LGK-974
- RSPO1
+ RSPO1
I
Patient 1
Patient 2
% OFE (normalized to Unt + RSPO1 sample)
Unt
Control CM
Wnt3a CM
Control CM + LGK-974
Wnt3a CM + LGK-974
LGK-974
- RSPO1
+ RSPO1
J
Unt
CHIR99021
LGK-974
K
OFE Quantification
% OFE (normalized to Unt sample)
Organoid Size
Organoid Diameter / µm
Unt
CHIR99021
LGK-974

Figure 1: WβS is essential for organoid regeneration and is driven by unidentified WNT(s).

(A) *Validation of hFT organoid culture and its relevance to hFT tissue.*

(B) *WβS activation (RSPO1) and suppression of TGF-β signaling (A83.01) are essential for stem cell renewal in organoids. EpCAM+ CD45- cells were FACS isolated from dissociated patient-derived FT tissue and cultured under the conditions shown. Images taken on day 12.*

(C) *Quantification of images in (B). Red arrow points to culture conditions of the reported method for culturing FT organoids.*

(D) *hFT and mOV organoids emerge from a single multipotent stem cell. Sorted EpCAM+ CD45- cells were cultured as single cells in single wells of 96-well plates. 0.5-1% of cells formed organoids that gradually increased in size and complexity, as shown. Formed organoids contained PAX8+ secretory cells and TUBB4+ ciliated cells, evidencing multipotency of the organoid-forming cell.*

(E) *Graphical summary of the experimental approaches employed to biomark and characterize putative FT stem cells.*

(F) *RSPO1 cooperates with an endogenous WNT to drive organoid regeneration. Treatments done on passage 1 organoids from plating day. The CHIR99021 + IWP-2/LGK-974 samples show that lack of organoid regeneration in LGK-974 / IWP-2-treated samples is due to WNT inhibition and not inhibitor toxicity.*

(G) *Quantification of images in (F), shown for three patient replicates. 19K cells, 12K cells or 7K cells were plated per sample for patients 1, 2 or 3, respectively.*

(H) *WNT3A fails to rescue inhibition of WNT-blocked organoids. Treatments done on passage 1 organoids.*

(I) *Quantification of images in (H), shown for two patient replicates. CM is conditioned medium. Activity of WNT3A CM was confirmed by the Wnt reporter (TOPFlash) assay (Figure S3A).*

(J) *mOV organoids regenerate independently of mouse WNTs.*

(K) *Quantification of OFE (left panel) and organoid size (right panel) of images shown in (J).*

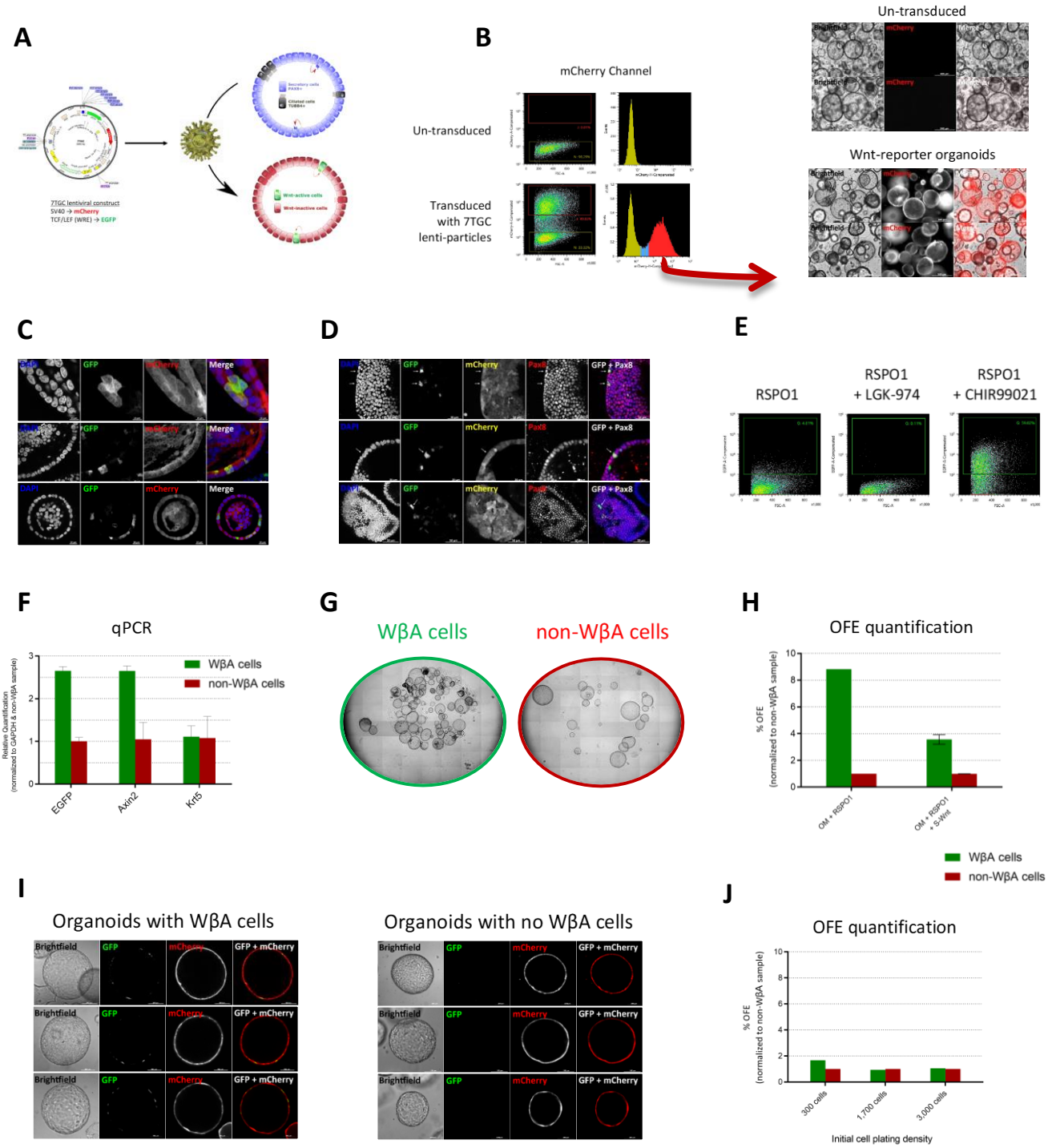
A
7TGC lentiviral construct
5V40 → mCherry
TCF/LEF (WRE) → EGFP
B
mCherry Channel
Un-transduced
Transduced with 7TGC lenti-particles
Un-transduced
Wnt-reporter organoids
C
D
E
RSPO1
RSPO1 + LGK-974
RSPO1 + CHIR99021
F
qPCR
WβA cells
non-WβA cells
EGFP
Axin2
Krt5
G
WβA cells
non-WβA cells
H
OFE quantification
% OFE (normalized to non-WβA sample)
OM + RSPO1
OM + RSPO1 + S/Wnt
WβA cells
non-WβA cells
I
Organoids with WβA cells
Organoids with no WβA cells
Brightfield
GFP
mCherry
GFP + mCherry
J
OFE quantification
% OFE (normalized to non-WβA sample)
300 cells
1,700 cells
3,000 cells
Initial cell plating density

Figure 2: WβA cells drive organoid regeneration.

(A) *Organoids were transduced with viral lenti-particles generated using the 7TGC construct (see Methods for details), which enables mCherry expression under a general (SV40) promoter and EGFP under TCF/LEF elements, also called WβS-Reporter Elements (WβS-RE).*

(B) *Transduced cells were selected by FACS and expanded using the optimised organoid culture conditions. Left panel shows FACS plots. Right panel shows images of organoids after 1 week of culture. Data representative of 4 patient replicates.*

(C) *Confocal imaging of WβS-reporter organoids post-fixation, showing WβA (EGFP+) cells.*

(D) *WβA (EGFP+) cells co-localize with PAX8, indicating WβA cells have a secretory cell lineage.*

(E) *Proportion of WβA cells increases upon WβS activation (CHIR99021) and is abolished upon WβS inhibition (LGK-974).*

(F) *WβA (EGFP+) cells express elevated levels of endogenous AXIN2, a marker of WβS activation.*

(G) *WβA cells are enriched in organoid formation ability. EGFP+ and EGFP- cells were FACS isolated and cultured for 10-13 days.*

(H) *Quantification of images in (I). OM + RSPO1 + SWNT treatments shown for two biological replicates. OFE is organoid formation efficiency.*

(I) *Live imaging of mOV WβS-reporter organoids. In contrast to hFT WβS-reporter organoids, mouse organoid culture is composed of organoids that contain (left panel) or lack (right panel) WβA cells.*

(J) *Quantification of OFE in mOV WβA vs non-WβA cells. mOV WβA cells are not enriched in organoid formation ability.*

A

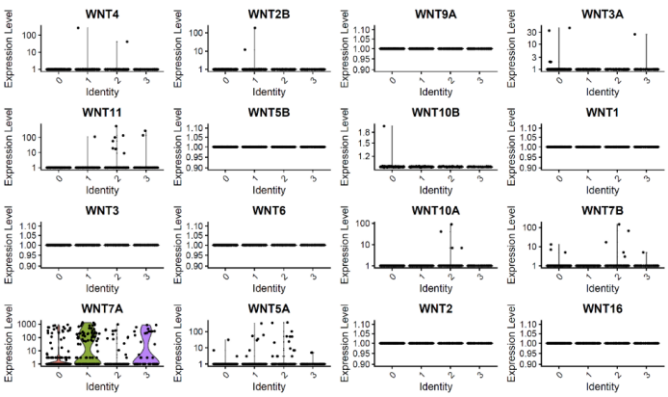

B

RNA FISH – hFT organoids

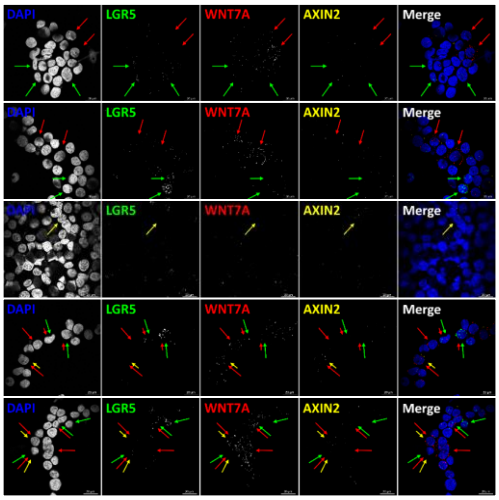

C

RNA FISH – mOV organoids

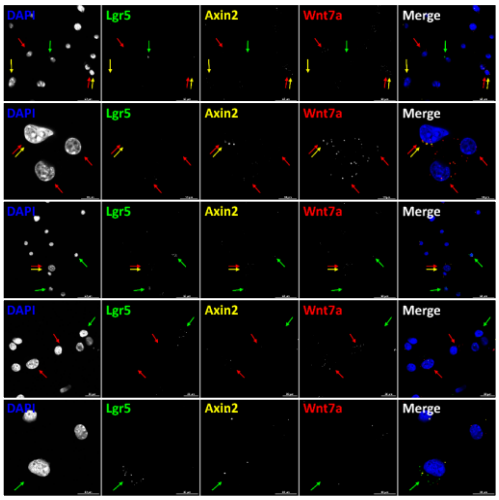

D

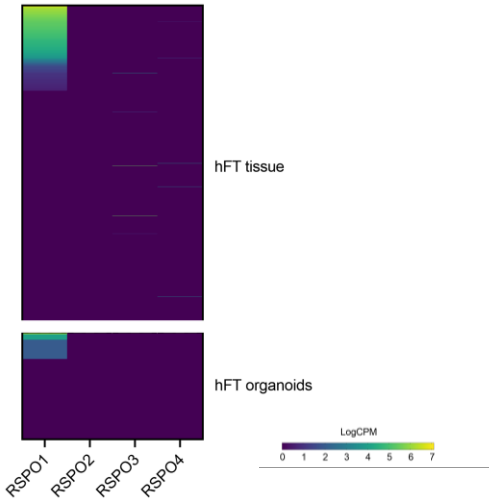

E

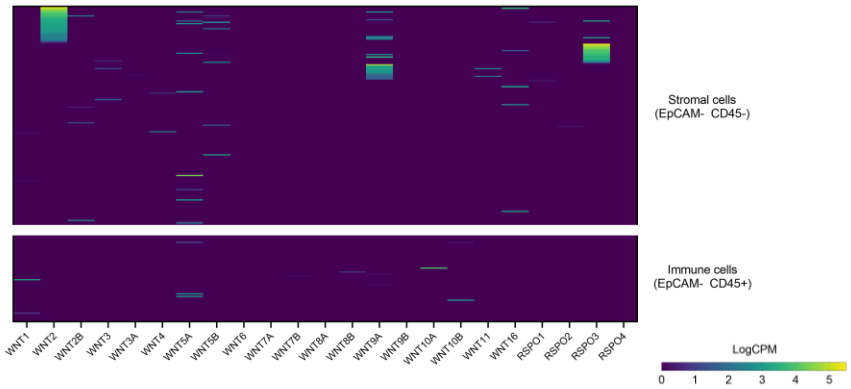

Figure 3: WNT7A is the WNT ligand that cooperates with RSPO1 to drive WβS and renewal of hFT organoids.

(A) *Single cell expression profile of the WNT family of ligands in hFT organoids. Based on SCT data, the frequency of WNT7A+ cells is ~ 5% in hFT tissue and ~20% in hFT organoids.*

(B) *Confirmation of WNT7A+ cells in hFT organoids. WNT7A+ cells may or may not co-express markers of WβS activation AXIN2 and LGR5. AXIN2+ cells and LGR5+ cells are largely distinct. Organoids were dissociated, cytospinned and fixed prior to RNA FISH staining.*

(C) *Confirmation of Wnt7a+ cells in mOV organoids. As in the human setting, Axin2+ cells here are distinct from Lgr5+ cells. Organoids were dissociated, cytospinned and fixed prior to RNA FISH staining.*

(D) *Heatmap showing the single cell expression profile of the R-Spondin family of proteins in hFT tissue and organoids. Every row represents a single cell.*

(E) *Heatmap showing the single cell expression profile of the WNT & R-Spondin family of ligands in the non-epithelial compartments of hFT tissue. Stromal and immune cells were FACS isolated using the antibodies shown.*

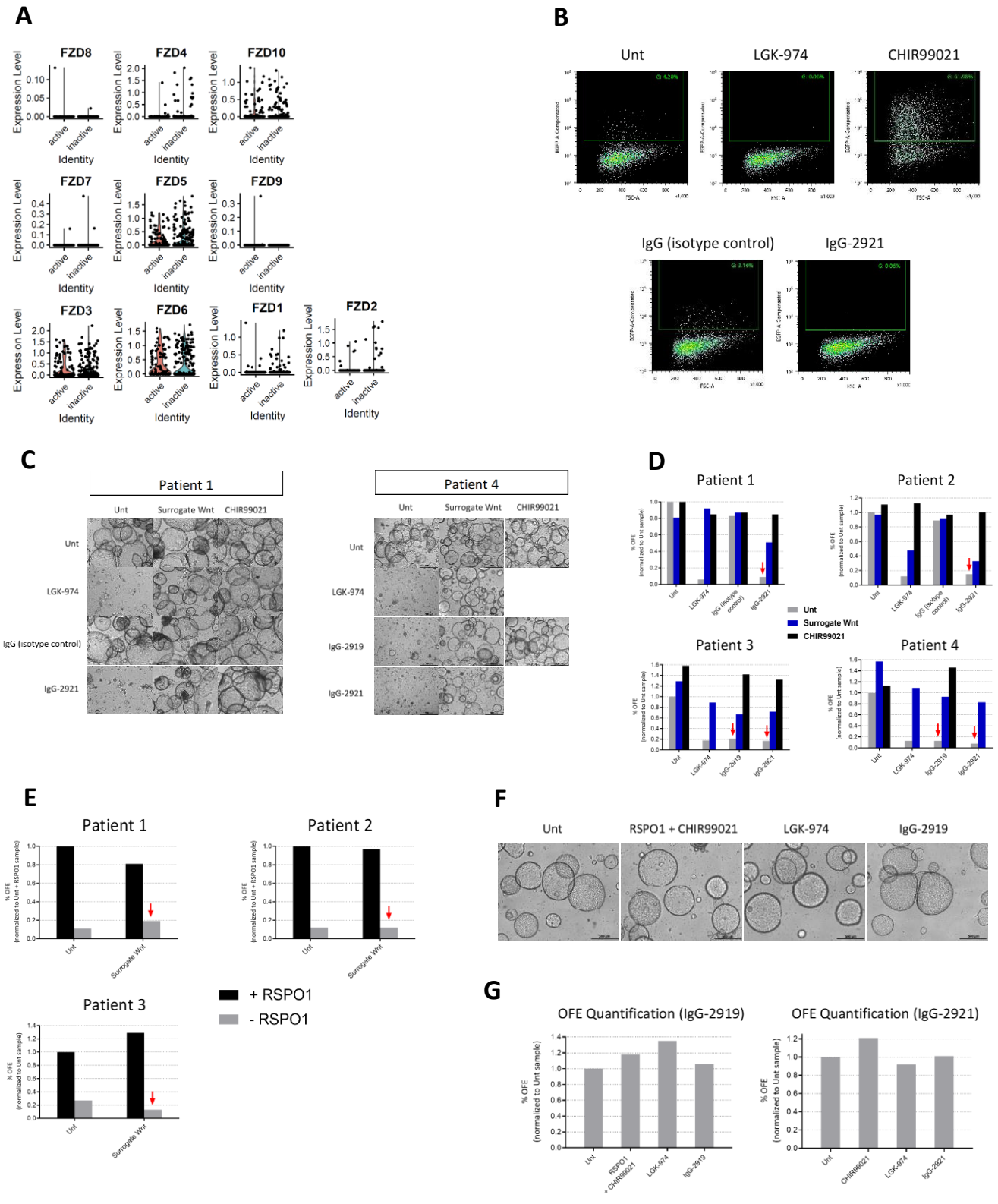
A
FZD8
FZD4
FZD10
FZD7
FZD5
FZD9
FZD3
FZD6
FZD1
FZD2
Expression Level
active
inactive
Identity
B
Unt
LGK-974
CHIR99021
IgG (isotype control)
IgG-2921
C
Patient 1
Patient 4
Unt
Surrogate Wnt
CHIR99021
LGK-974
IgG (isotype control)
IgG-2921
IgG-2919
D
Patient 1
Patient 2
Patient 3
Patient 4
% OFE
(normalized to Unt sample)
Unt
Surrogate Wnt
CHIR99021
E
Patient 1
Patient 2
Patient 3
% OFE
(normalized to Unt + RSPO1 sample)
(normalized to Unt sample)
Unt
Surrogate Wnt
+ RSPO1
- RSPO1
F
Unt
RSPO1 + CHIR99021
LGK-974
IgG-2919
G
OFE Quantification (IgG-2919)
OFE Quantification (IgG-2921)
% OFE
(normalized to Unt sample)
Unt
RSPO1 + CHIR99021
LGK-974
IgG-2919
IgG-2921

Figure 4: FZD5 is the WNT7A receptor.

(A) *Single cell expression profile of the FZD family of receptors in hFT organoids.*

(B) *Anti-FZD5 IgG-2921 depletes % of WβA cells in WβS-reporter organoids, phenocopying the effect of blocking WNT secretion. Organoids used here were mOV.*

(C) *Anti-FZD5 antibodies (IgG-2921 and IgG-2919) reduce OFE by 80-90%, phenocopying the effect seen in WNT-blocked organoids (LGK-974). Treatments done on passage 1 organoids.. Images taken on day 12.*

(D) *Quantification of images shown in (D) as well as for other patient replicates. Red arrows point to organoid inhibition due to FZD5 blocking.*

(E) *Surrogate Wnt drives organoid regeneration in a FZD-specific, RSPO1-sensitive manner. Treatments done on passage 1 organoids.*

(F) *mOV organoids are unaffected by blocking FZD5 receptor. Representative images shown on day 10.*

(G) *Quantification of images shown in (F, left panel) as well as for another replicate using a different anti-FZD5 IgG (IgG-2921).*

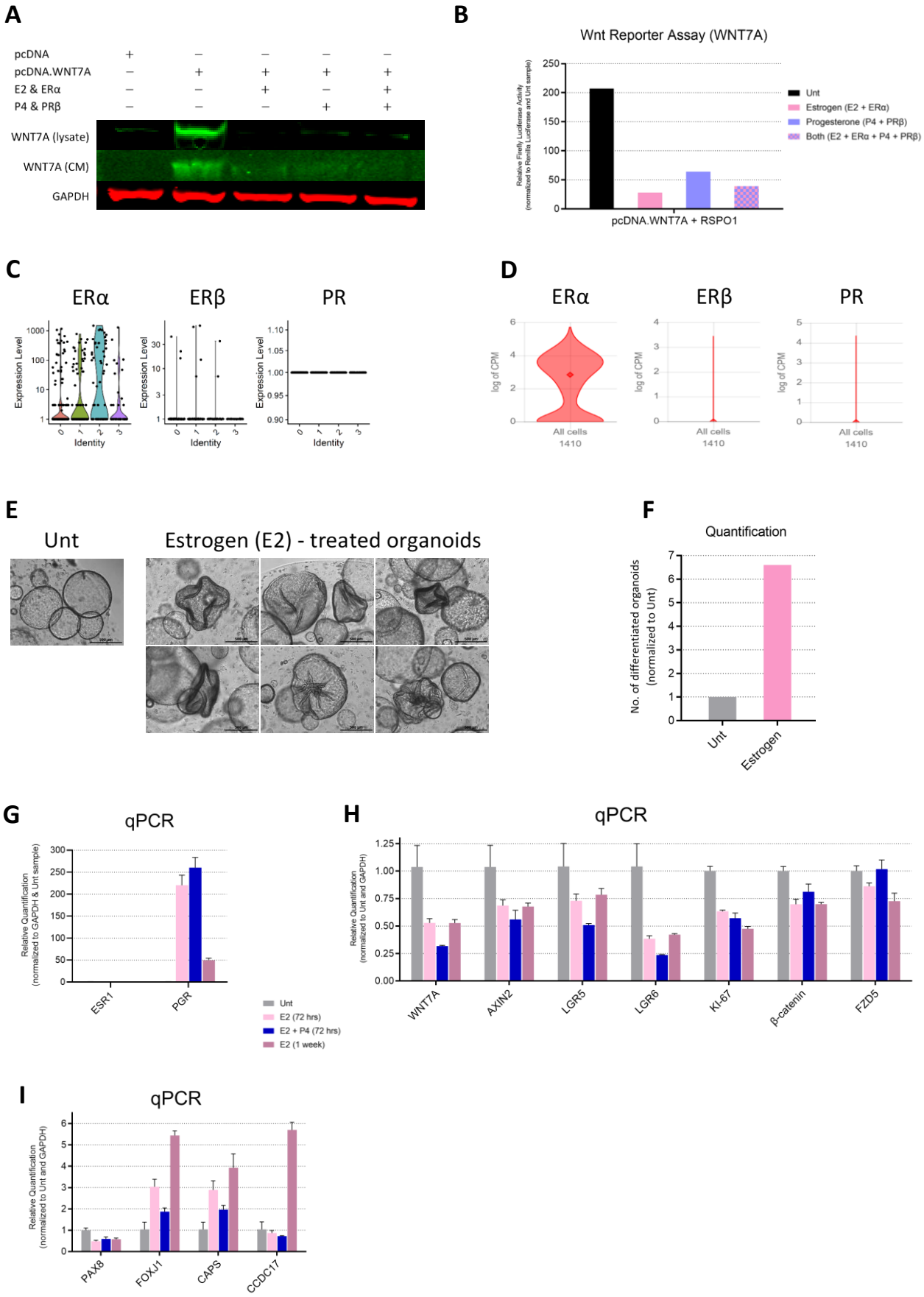
A
pcDNA
pcDNA.WNT7A
E2 & ERα
P4 & PRβ
WNT7A (lysate)
WNT7A (CM)
GAPDH
B
Wnt Reporter Assay (WNT7A)
Relative Firefly Luciferase Activity (normalized to Renilla Luciferase and Unt sample)
pcDNA.WNT7A + RSPO1
Unt
Estrogen (E2 + ERα)
Progesterone (P4 + PRβ)
Both (E2 + ERα + P4 + PRβ)
C
ERα
ERβ
PR
Expression Level
Identity
D
ERα
ERβ
PR
log of CPM
All cells
1410
E
Unt
Estrogen (E2) - treated organoids
F
Quantification
No. of differentiated organoids (normalized to Unt)
Unt
Estrogen
G
qPCR
Relative Quantification (normalized to GAPDH & Unt sample)
ESR1
PGR
Unt
E2 (72 hrs)
E2 + P4 (72 hrs)
E2 (1 week)
H
qPCR
Relative Quantification (normalized to Unt and GAPDH)
WNT7A
AXIN2
LGR5
LGR6
KI-67
β-catenin
FZD5
I
qPCR
Relative Quantification (normalized to Unt and GAPDH)
PAX8
FOXJ1
CAPS
CCDC17

Figure 5: Estrogen suppresses WNT7A and promotes differentiation of hFT organoids.

(A) *Estrogen & Progesterone downregulate WNT7A protein. HEK293 cells were transfected with 1 µg of the indicated constructs. Cells were treated with 17β-estradiol (E2), progesterone (P4) or both for 72 hrs, at 100 nM (E2) or 1µM (P4). Western Blot shows cytoplasmic (lysate) and secreted (conditioned medium, CM) WNT7A protein levels.*

(B) *Estrogen & Progesterone downregulate WNT7A activity. All samples were transfected with WNT7A construct. WNT7A-induced TOPFlash signal is reduced by 90% upon Estrogen treatment in HEK293 cells. ERα and PRβ were transfected at 200 ng per well. E2 and P4 were administered at the concentrations indicated in (A). Data is representative of two biological replicates.*

(C) *Single cell transcriptomic profile of hormone receptor expression in hFT organoids. ERα is the predominant Estrogen receptor expressed. As expected, Progesterone Receptor (PR) is not expressed, as its expression is regulated by Estrogen. Organoids were not treated with Estrogen prior to scRNA sequencing.*

(D) *Single cell transcriptomic profile of hormone receptor expression in hFT tissue. This mirrors expression seen in organoids.*

(E) *Estrogen treatment of organoids triggers pronounced morphological changes within 72 hours, producing dark staining, crippled organoids with extensive internal folding and invaginations.*

(F) *Quantification of images in (E).*

(G) *Estrogen treatment of hFT organoids induces PR expression, a classic E2-ER target gene.*

(H) *Estrogen suppresses WNT7A transcription in organoids. This is accompanied by a reduction in WβS activation marker AXIN2. Progesterone does not antagonize these changes.*

(I) *Estrogen promotes differentiation of hFT organoids, triggering a reduction in secretory cell marker (PAX8) and an increase in ciliated cell markers. CCDC17, a ciliated cell marker recently identified using scRNA-seq of fresh hFT tissue (Hu et al., 2020), is activated in long-term but not short-term Estrogen-treated organoids. Data in (E-I) are for the same samples, and E2 (1 week) treatment is normalized to Unt (1 week) control sample not shown for simplicity.*

A

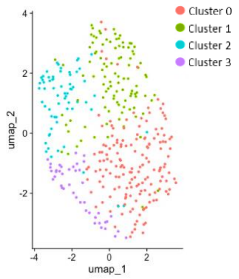

B

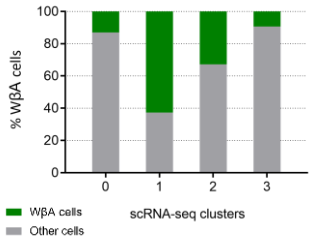

C

	Cluster 0	Cluster 2	Cluster 3
Cluster 1 (WβA)	< 0.0001	0.0002	< 0.0001
Cluster 2	0.0011		0.0051
Cluster 3	0.6092		

D

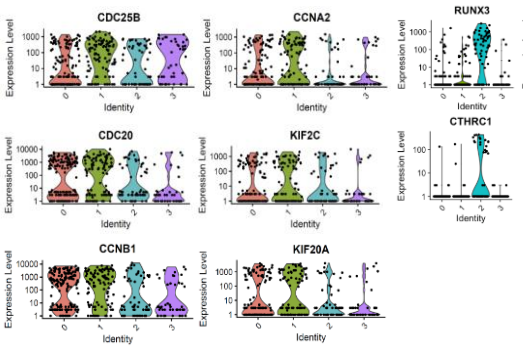

E

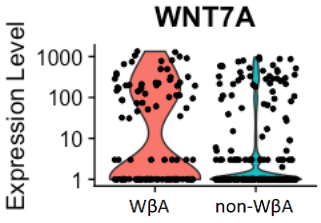

F

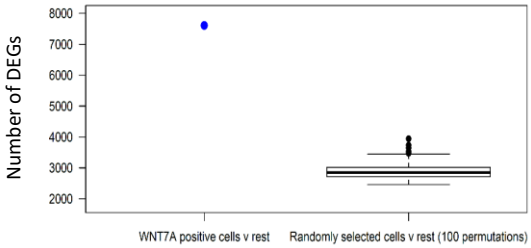

G

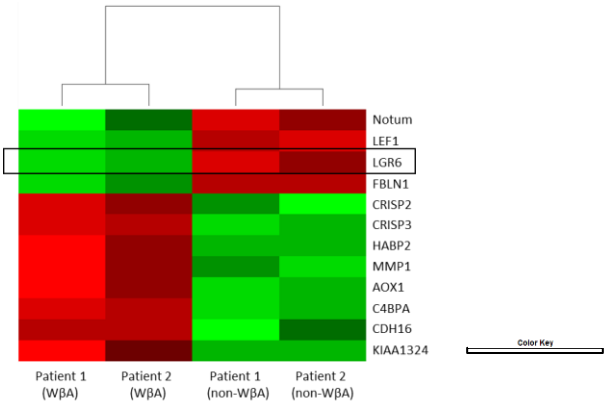

H

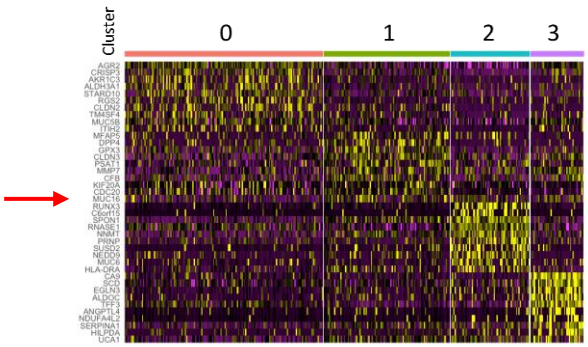

Figure 6: Single cell transcriptomic analysis of WβA cells.

(A) *De novo clustering of cells after cell cycle correction, showing hFT organoids are composed of 4 transcriptomic clusters of cells.*

(B) *Majority of WβA cells concentrate in Cluster 1.*

(C) *P-values from pairwise Fisher's test comparisons between all clusters, showing enrichment of WβA cells in Cluster 1 is statistically significant.*

(D) *The WβA cluster is proliferative and enriched in various G2-to-M cell cycle transition regulators.*

(E) *WNT7A expression is enriched in WβA cells.*

(F) *WNT7A+ cells have unique transcriptomes. The figure shows the number of differentially expressed genes (DEGs) obtained by comparing the transcriptomes of WNT7A+ cells versus WNT7A- cells. To ensure the number of DEG's between WNT7A+ and WNT7A- cells is not due to stochastic cell-to-cell differences, multiple control analyses were performed between two randomly selected groups of WNT7A- cells, each containing the same number of cells as the WNT7A+ group.*

(G) *Selected DEGs from bulk transcriptomic analysis of WβA versus non-WβA cells.*

(H) *Heatmap showing marker genes for each cluster. The WβA cluster is marked by CA125 (red arrow), a clinical marker of HGSOC diagnosis, progression and response to therapy.*

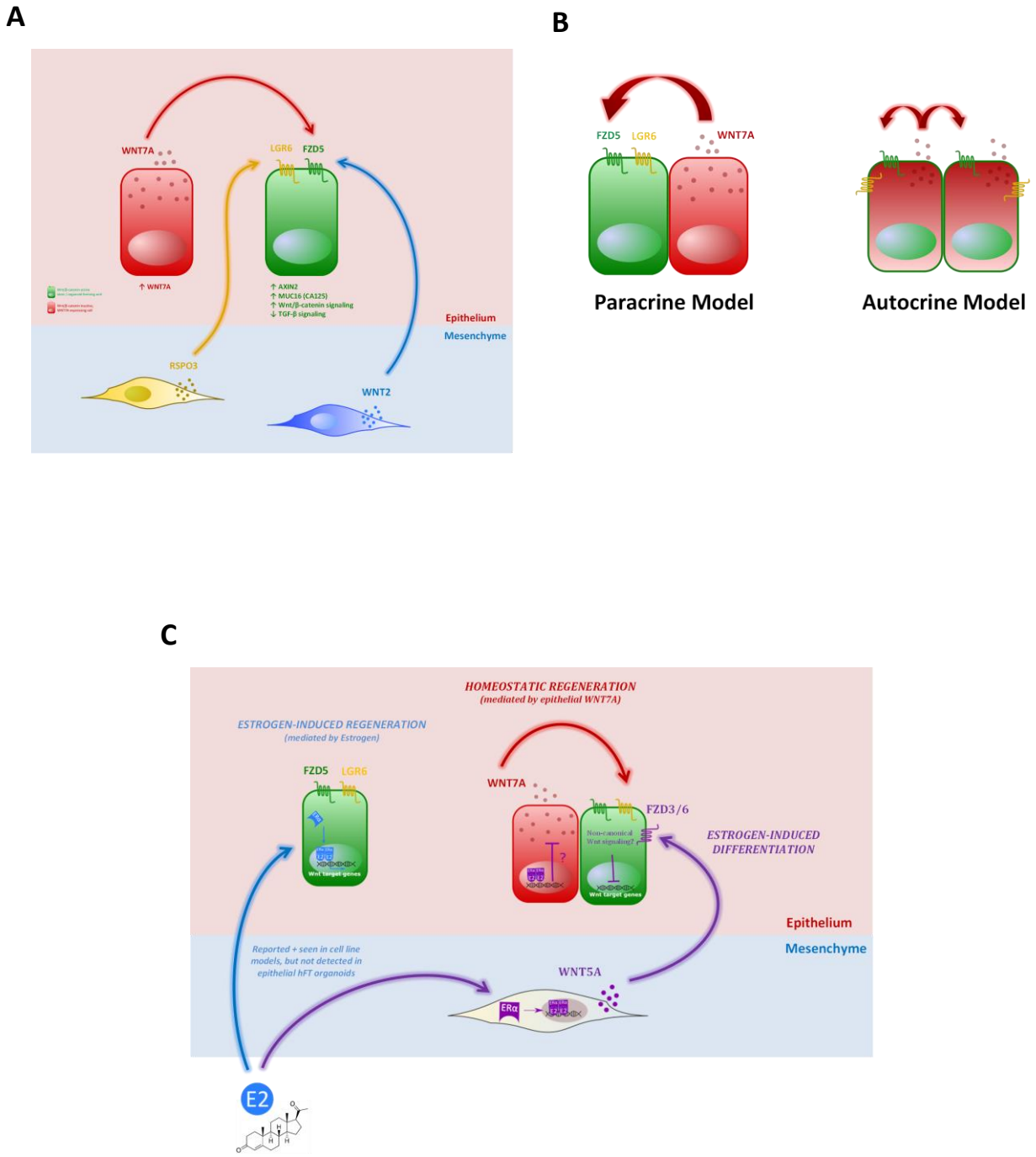

Figure 7: Working model on the molecular maintenance and hormonal regulation of the FT stem cell niche.